



A 1-km global dataset of historical (1979-2017) and future (2020-2100) Köppen-Geiger climate classification and bioclimatic variables

Diyang Cui¹, Shunlin Liang¹, Dongdong Wang¹, Zheng Liu¹

¹Department of Geographical Sciences, University of Maryland, College Park, 20740, USA

5 *Correspondence to:* Shunlin Liang(sliang@umd.edu)

Abstract.

The Köppen-Geiger classification scheme provides an effective and ecologically meaningful way to characterize climatic conditions and has been widely applied in climate change studies. Significant changes in Köppen climates have been observed and projected in the recent two centuries. Current accuracy, temporal coverage, spatial and temporal resolution of historical and future climate classification maps cannot sufficiently fulfil the current needs of climate change research. Comprehensive assessment of climate change impacts requires a more accurate depiction of fine-grained climatic conditions and continuous long-term time coverage. Here, we present a series of improved 1-km Köppen-Geiger climate classification maps for ten historical periods in 1979-2017 and four future periods in 2020-2099 under RCP2.6, 4.5, 6.0, and 8.5. The historical maps are derived from multiple downscaled observational datasets and the future maps are derived from an ensemble of bias-corrected downscaled CMIP5 projections. In addition to climate classification maps, we calculate 12 bioclimatic variables at 1-km resolution, providing detailed descriptions of annual averages, seasonality, and stressful conditions of climates. The new maps offer higher classification accuracy and demonstrate the ability to capture recent and future projected changes in spatial distributions of climate zones. On regional and continental scales, the new maps show accurate depictions of topographic features and correspond closely with vegetation distributions. We also provide a heuristic application example to detect long-term global-scale area changes of climate zones. This high-resolution dataset of Köppen-Geiger climate classification and bioclimatic variables can be used in conjunction with species distribution models to promote biodiversity conservation and to analyze and identify recent and future interannual or interdecadal changes in climate zones on a global or regional scale. The dataset referred to as KGClim, is publicly available at <http://doi.org/10.5281/zenodo.4546140> for historical climate and <http://doi.org/10.5281/zenodo.4542076> for future climate.

25 1 Introduction

Climate has direct impacts on the processes and functioning of the ecosystem as well as on the distribution of species. (Chen, Hill, Ohlemüller, Roy, & Thomas, 2011; Ordonez & Williams, 2013; Pinsky, Worm, Fogarty, Sarmiento, & Levin, 2013; Thuiller, Lavorel, Araújo, Sykes, & Prentice, 2005). The spatial patterns of climates have been often identified using the Köppen climate classification system (Köppen, 1931).



30 The Köppen classification system was designed to map the distribution of the world's biomes based on the annual cycles of surface air temperature and precipitation (Köppen, 1936). Compared with other human expertise based climate mapping methods (e.g., Holdridge, 1947; Thornthwaite, 1931; Walter & Elwood, 1975) and clustering approaches (e.g., Netzel & Stepinski, 2016), which suffer from a lack in meteorological basis, the Köppen classification demonstrates stronger correlation with distributions of biomes and soil types (Bockheim, Gennadiyev, Hammer, & Tandarich, 2005; Rohli, Joyner, Reynolds, & Ballinger, 2015). It provides an ecologically relevant and effective method to classify climate conditions by combining seasonal cycles of surface air temperature and precipitation (Cui, Liang, & Wang, 2021).

The Köppen classification has been widely applied in biological science, earth and planetary sciences, and environmental science (Rubel & Kottek, 2011). It is a convenient and integrated tool to identify spatial patterns of climate distributions and to examine relationships between climates and biological systems. It has been found useful for a variety of issues on climate change, such as hydrological cycle studies (Peel, McMahon, Finlayson, & Watson, 2001), Arctic climate change (Feng et al., 2012; Wang & Overland, 2004), assessment of climate change impacts on ecosystem (Roderfeld et al., 2008), biome distribution (Rohli, Joyner et al., 2015) and biodiversity (Garcia, Cabeza, Rahbek, & Araújo, 2014).

There has been a resurgence in the application of the Köppen climate classification in climate change research over the recent decades (Cui, Liang, & Wang, 2021). The Köppen climate classification has been used to set up dynamic global vegetation models (Poulter et al., 2011), to characterize species composition (Brugger & Rubel, 2013), to model the species range distribution (Brugger & Rubel, 2013; Tererai & Wood, 2014; Webber et al., 2011), and to analyze the species growth behavior (Tarkan & Vilizzi, 2015). The Köppen classification has also been applied to detect the shifts in geographical distributions of climate zones (Belda, Holtanová, Kalvová, & Halenka, 2016; Chan & Wu, 2015; Feng et al., 2014; Mahlstein, Daniel, & Solomon, 2013). It also has the potential to aggregate climate information on warmth and precipitation seasonality into ecologically important climate classes thereby simplifying spatial variability. This climate classification system adds a new direction to develop climate change metrics and can provide support for the growth of species distribution modelling (SDM).

The recent Köppen climate classification maps have a resolution ranging between 0.5° and 1-km (Cui, Liang, & Wang, 2021). Early published Köppen climate classification maps have a relatively low resolution of 0.5° (Belda, Holtanová, Halenka, & Kalvová, 2014; Grieser, Gommès, Cofield, & Bernardi, 2006; Kottek, Grieser, Beck, Rudolf, & Rubel, 2006; Kriticos et al., 2012; Rubel & Kottek, 2010). Several map products used interpolation methods to obtain a higher resolution of ~0.1° (Kriticos et al., 2012; Peel, Finlayson, & McMahon, 2007; Rubel, Brugger, Haslinger, & Auer, 2017). Fine resolutions of at least 1-km are required to detect microrefugia and promote effective conservation. Recently, Beck et al. (2018) generated new global climate classification maps for two periods 1980-2016 and 2071-2100 under RCP8.5 with a resolution of 1-km. To represent historical climates, they adjusted the inconsistent temporal spans of climatology datasets to the period 1980-2016, by adding interpolated temperature change offsets or multiplying precipitation factors, which may lead to biased coverage of the historical period. Current classification accuracy, temporal coverage, spatial and temporal resolution of historical and future climate



classification maps cannot sufficiently fulfil the current needs of climate change research. Significant changes in Köppen climates have been observed and projected in the recent two centuries (Belda et al., 2014; Chan & Wu, 2015; Chen & Chen, 2013; Rohli, Andrew, Reynolds, Shaw, & Vázquez, 2015; Yoo & Rohli, 2016). Previous studies found that large-scale shifts
65 in climate zones have been observed over more than 5% of the total land area since the 1980s, and approximately 20.0% of the total land area is projected to experience climate zone changes under RCP8.5 by 2100 (Cui, Liang, & Wang, 2021). Detection of recent and future changes in climate zones with the application of Köppen climate maps needs more accurate depiction of fine-grained climatic conditions, continuous and longer temporal coverage.

This creates the urgent need for global maps of Köppen climate classification with increased accuracy, finer spatial and
70 temporal resolutions. Currently available global observational datasets of temperature and precipitation collected during the recent centuries, and the global climate simulations under alternative future climate scenarios have offered the possibility to create a comprehensive dataset for past and future climates. In this study, we presented an improved long-term climate classification map series for 1) ten historical 30-yr periods of the observational record (1979-2008, 1980-2009...1988-2017) and four future 30-yr periods (2020-2049, 2040-2069, 2060-2089, 2070-2099) under four RCPs (RCP2.6, 4.5, 6.0 and 8.5).
75 To improve the classification accuracy and achieve a resolution as fine as 1-km (30 arc-second), we combined multiple datasets, including WorldClim V2 (Fick & Hijmans, 2017; Booth et al., 2014), CHELSA V1.2 (Booth et al., 2014), CRU TS v4.03 (New, Hulme, & Jones, 2000), UDEL (Willmott & Matsuura, 2001), GPCC datasets (Beck, Grieser, & Rudolf, 2005) and bias-corrected downscaled Coupled Model Intercomparison Project Phase 5 (CMIP5) model simulations (Navarro-Racines, Tarapues, Thornton, Jarvis, & Ramirez-Villegas, 2020) (Table 1). We also calculated 12 bioclimatic variables at the
80 same 1-km resolution using these climate datasets for the same historical and future periods. This dataset can be used to in conjunction with SDMs to promote biodiversity conservation, or to analyse and identify recent and future changes in climate zones on a global or regional scale.

To validate the Köppen-Geiger climate classification maps, we used the station observations from Global Historical Climatology Network-Daily (GHCN-D) (Menne, Durre, Vose, Gleason, & Houston, 2012), and Global Summary Of the Day (GSOD) (National Climatic Data Center, NESDIS, NOAA, & U.S. Department of Commerce, 2015) database. At the regional
85 and continental scale, we compared our Köppen-Geiger climate classification maps with previous map products, associated maps of forest cover, and elevation distribution, for 1) regions with large spatial gradients in climates, including central and eastern Africa, Europe, North America, and 2) regions with sharp elevation gradients, including Tibetan Plateau, central Rocky Mountains, central Andes. Further, we conducted sensitivity analysis with respect to classification temporal scale, dataset
90 input, and data integration methods. We also provided a heuristic example which used climate classification map series to detect the long-term area changes of climate zones, showing how the Köppen-Geiger climate classification map series can be applied in climate change studies.



2 Datasets

Table 1 Climatology datasets to generate present global maps of Köppen climate classification with varied spatial resolutions

Dataset	Spatial Resolution	Temporal Span	Variable(s)	Source and Description
Present Köppen classification map series with resolution of 30 arc-second (1km)				
CRU	0.5°	1979-2017	T	Climatic Research Unit (CRU) TS v4.03
UDEL	0.5°	1979-2017	T, P	U. of Delaware Precipitation and Air Temperature
WorldClim	0.0083°	1970-2000	T, P	WorldClim Historical Climate Data V2
CHELSA	0.0083°	1979-2013	T, P	Climatologies at high resolution for the earth's land surface areas (CHELSA)
GPCC	0.5°	1979-2016	P	Global Precipitation Climatology Centre (GPCC)
Future Köppen classification map series with resolution of 30 arc-second (1km)				
CMIP5	0.0083°	2020-2100	T, P	CCAFS-Climate Statistically Downscaled Delta Method CMIP5 data
WorldClim	0.0083°	1970-2000	T, P	WorldClim Historical Climate Data V2

Table 1 lists the climatology datasets with global coverage and on a monthly time step, used to generate historical and future
 95 Köppen-Geiger climate map series. The present 1-km Köppen-Geiger classification map series for 1979-2017 was derived
 from the Climatologies at High-resolution for the Earth's Land Surface Areas (CHELSA) V1.2 (Karger et al., 2017),
 WorldClim Historical Climate Data V2 (Fick & Hijmans, 2017; Booth et al., 2014) and the statistically downscaled Climatic
 Research Unit (CRU) TS v4.03 (New et al., 2000), University of Delaware Precipitation and Air Temperature (UDEL)
 (Willmott & Matsuura, 2001) and Global Precipitation Climatology Centre (GPCC) (Beck et al., 2005) datasets. To decide the
 100 datasets to use, we conducted a sensitivity analysis on the input climatology datasets and utilized monthly air temperature
 datasets from CRU, UDEL, GHCN_CAMS Gridded 2m Temperature (Fan & Dool, 2008) and monthly precipitation datasets
 from GPCC, UDEL, NOAA's PRECipitation REConstruction over Land (PREC/L) (Chen, Xie, Janowiak, & Arkin, 2002).
 Evaluation results indicated that incorporating only CRU, UDEL temperature datasets and UDEL, GPCC precipitation datasets
 led to higher accuracy in the classification results. Therefore, we chose CRU, UDEL, and GPCC datasets as the classification
 105 system input to boost the final accuracy.

To explicitly correct topographic effect, we used 1-km CHELSA V1.2 and WorldClim V2 datasets in addition to the 0.5°
 resolution datasets. The CHELSEA dataset statistically downscaled temperature data from the ERA-Interim climatic reanalysis.
 For precipitation data, it incorporated multiple orographic predictors and performed bias correction (Karger et al., 2017). With
 major topo-climatic drivers considered, the CHELSA dataset demonstrated good performance in ecological science studies.
 110 CHELSA data exhibited comparable accuracy for temperatures and better predicted precipitation patterns based on the
 validation results (Karger et al., 2017).

We produced the future Köppen classification map series using the CCAFS climate statistically bias-corrected and downscaled
 CMIP5 projections (Navarro-Racines et al., 2020). The CCAFS presented a global database of future climates developed by
 a climate model bias correction method based on the CMIP5 GCM simulations (Taylor, Stouffer, & Meehl, 2012) archive,



115 coordinated by the World Climate Research Programme in support of the IPCC Fifth Assessment Report (AR5) (Hartmann et al., 2013). The total is 35 GCMs, and all RCPs, RCP 2.6, 4.5, 6.0 and 8.5 (Table S1). Projections are available at varied coarse scales (70–400km). To achieve high-resolution (1km) climate representations, downscaling method has been applied with the use of the WorldClim data (Fick & Hijmans, 2017; Booth et al., 2014). Technical evaluation showed that the bias-correction method that CCAFS data applied reduced climate model bias by 50–70%, which could potentially address the bias issue in
 120 model simulations for the threshold-based Köppen classification scheme.

3 Methodology

3.1 Köppen-Geiger climate classification

Table 2 Criteria of Köppen-Geiger climate classification with temperature in oC and precipitation in mm.

1st	2nd	3rd	Description	Criterion
A			Tropical	Not (B) & $T_{cold} \geq 18$
	f		- Rainforest	$P_{dry} \geq 60$
	m		- Monsoon	Not (Af) & $P_{dry} \geq 100 - MAP/25$
	w		- Savannah	Not (Af) & $P_{dry} < 100 - MAP/25$
B			Arid	$MAP < 10 \times P_{threshold}$
	W		- Desert	$MAP < 5 \times P_{threshold}$
	S		- Steppe	$MAP \geq 5 \times P_{threshold}$
		h	-- Hot	$MAT \geq 18$
		k	-- Cold	$MAT < 18$
C			Temperate	Not (B) & $T_{hot} > 10$ & $-3 < T_{cold} < 18$
	w		- Dry winter	$P_{wdry} < P_{swe}/10$
	s		- Dry summer	Not (w) & $P_{sdry} < 40$ & $P_{sdry} < P_{wwet}/3$
	f		- Without dry season	Not (s) or (w)
		a	-- Hot summer	$T_{hot} \geq 22$
		b	-- Warm summer	Not (a) & $T_{mon10} \geq 4$
	c	-- Cold summer	Not (a or b) & $1 \leq T_{mon10} < 4$	
D			Boreal	Not (B) & $T_{hot} > 10$ & $T_{cold} \leq -3$
	w		- Dry winter	$P_{wdry} < P_{swe}/10$
	s		- Dry summer	Not (w) & $P_{sdry} < 40$ & $P_{sdry} < P_{wwet}/3$
	f		- Without dry season	Not (s) or (w)
		a	- Hot summer	$T_{hot} \geq 22$
		b	- Warm summer	Not (a) & $T_{mon10} \geq 4$
		c	- Cold summer	Not (a), (b) or (d)
		d	- Very cold winter	Not (a) or (b) & $T_{cold} < -38$
E			Polar	Not (B) & $T_{hot} \leq 10$



T	- Tundra	$T_{hot} > 0$
F	- Frost	$T_{hot} \leq 0$

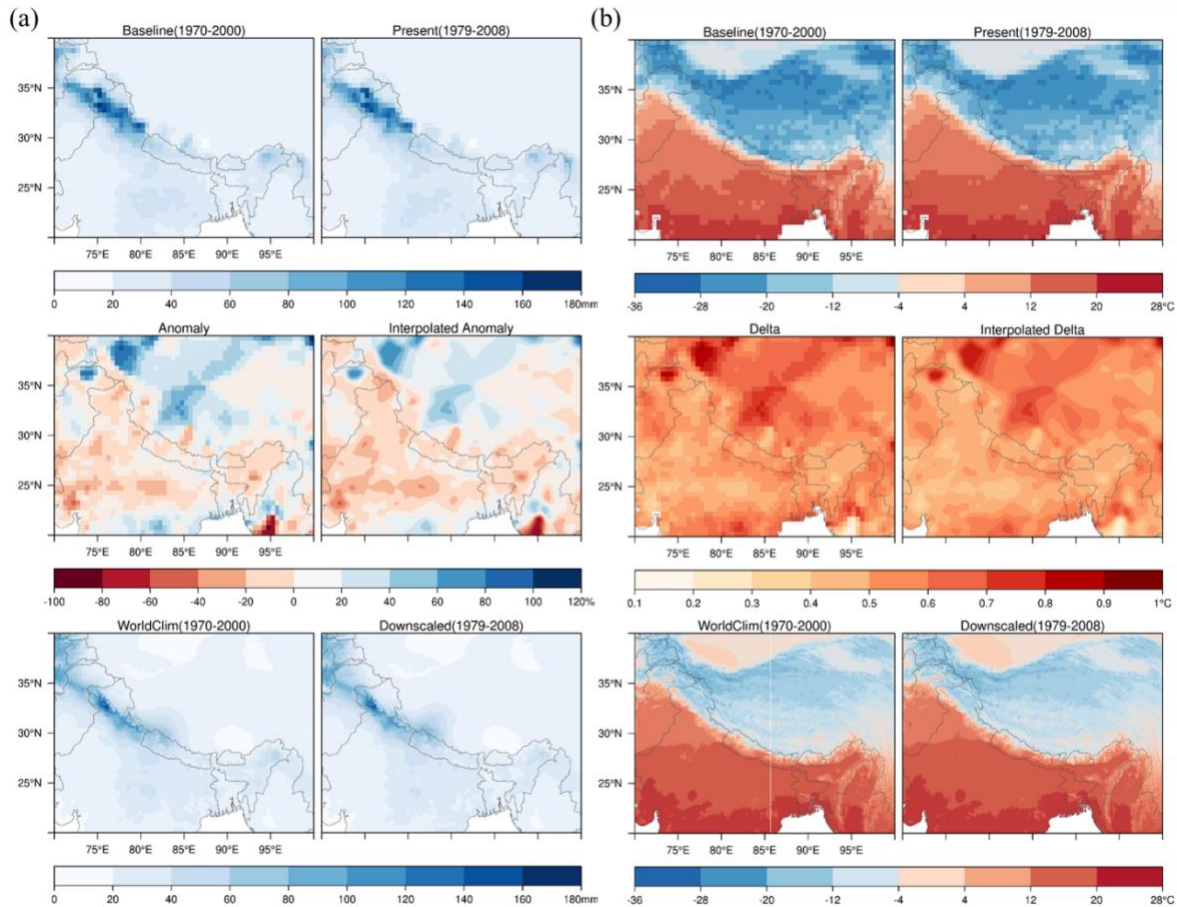
MAT = mean annual air temperature ($^{\circ}C$); T_{cold} = the air temperature of the coldest month ($^{\circ}C$); T_{hot} = the air temperature of the warmest month ($^{\circ}C$); T_{mon10} = the number of months with air temperature $> 10^{\circ}C$; MAP = mean annual precipitation (mm y^{-1}); P_{dry} = precipitation in the driest month (mm $month^{-1}$); P_{sdry} = precipitation in the driest month in summer (mm $month^{-1}$); P_{wdry} = precipitation in the driest month in winter (mm $month^{-1}$); P_{swet} = precipitation in the wettest month in summer (mm $month^{-1}$); P_{wwet} = precipitation in the wettest month in winter (mm $month^{-1}$); $P_{threshold} = 2 \times MAT$ if $> 70\%$ of precipitation falls in winter, $P_{threshold} = 2 \times MAT + 28$ if $> 70\%$ of precipitation falls in summer, otherwise $P_{threshold} = 2 \times MAT + 14$.

The Köppen climate classification scheme was first introduced by Wladimir Köppen in 1900. It is one of the earliest quantitative classification systems of Earth's climates. Its modification, Köppen-Geiger classification was first published in 1936 (Köppen, 1936), developed by Wladimir Köppen and Rudolf Geiger. KGC identifies climates based on their effects on plant growth from the aspects of warmth and aridity, and classifies climate into five main climate classes and 30 subtypes (Rubel & Kottek, 2011). The five main climate zones distinguish between plants of the tropical climate zone (A), the arid climate zone (B), the temperate climate zone (C), the boreal climate zone (D) and the polar climate zone (E), referring to the five major climate zones (Sanderson, 1999). All these main climate zones are thermal zones except the arid (B) climate zone, which is defined based on precipitation threshold.

This research followed the Köppen-Geiger climate classification as described in Kottek et al. (2006), and Rubel & Kottek (2010). This latest version of the KGC scheme was first presented by Geiger (1961) (Table 2). Several existing Köppen-Geiger climate map products, including Peel et al. (2007), Kriticos et al. (2012), and Beck et al. (2018) applied the KGC scheme modified following Russell (1931). Russell (1931) adjusted the definition of the boundary of temperate (C) and boreal (D) climate zones using the coldest monthly temperature $> 0^{\circ}C$ instead of $> -3^{\circ}C$. This threshold was proposed because the $0^{\circ}C$ line fits the distribution of the topographical features and vegetation in western United States, where at that time meteorological stations were sparsely distributed (Jones, 1932). However, the application of $0^{\circ}C$ boundary to the global climates has not been validated. Therefore, this research didn't utilize the Russell's modification (1931) and followed the latest version KGC proposed by Geiger (1961).



140 3.2 Statistical downscaling



145 **Figure 1. Illustration of the downscaling process.** (a) Anomaly downscaling method with January total precipitation from GPCP dataset and (b) delta downscaling method with January temperature from CRU dataset. Baseline (1970-2000) and present-day climate data (e.g. 1979-2008) are from CRU, UDEL, or GPCP datasets, which have a coarse spatial resolution of 0.5°. Precipitation anomaly is change factor of monthly precipitation from baseline to present-day climates. Temperature delta is change in monthly air temperature from baseline to present-day climates. WorldClim (1970-2000) climate data is adjusted by multiplying 30 arc-second interpolated anomaly (for precipitation) or adding 30 arc-second interpolated delta (for temperature) to generate the downscaled climate surfaces with 30 arc-second resolution. Precipitation values in mm/month and temperature values in °C.

150 Due to limited number of available observational datasets with high resolution and long-term continuous temporal coverage, the research implemented the delta method by applying a delta change or change factor onto the WorldClim historical observations (Fick & Hijmans, 2017) to achieve 30-yr average climatology data with a 1-km resolution based on the CRU, UDEL and GPCP datasets. The delta method is a statistical downscaling method that assumes that the relationship between climatic variables remain relatively constant at local scale. We applied delta method to downscale the long-term (30-yr) mean climates using coarse-resolution monthly climatology datasets. The delta changes or change factors are calculated as the 155 differences between the 30-yr long-term means of temperature or precipitation of baseline (1970-2000) and present-day



climates. The delta method comprises the following four steps: 1) calculate 30-yr averages for baseline (1970-2000) and present day of monthly temperature and precipitation; 2) calculate anomaly for precipitation and delta for temperature; 3) apply thin-plate splines interpolation (TPS) to create 1km surface of precipitation anomaly and temperature delta; 4) multiply anomaly or add delta to historical climates based on WorldClim dataset (Fig. 1).

160 First, using monthly time series from CRU, UDEL and GPCC datasets, we calculated 30-yr means as a baseline (1970-2000),
for each climatology dataset and each variable. We used 1970-2000 as baseline period, for consistency with WorldClim
Historical Climate Data V2. Next, we calculated 30-yr means for each month and each 30-yr present-day period in 1979-2017.
We then calculated anomalies as proportional differences between present-day and baseline in total precipitation and delta as
165 difference in temperature. To derive 30 arc-second (1-km) anomaly or delta surfaces, we applied thin-plate splines (TPS)
interpolation (Craven & Wahba, 1978; Franke, 1982; Schempp, Zeller, & Duchon, 1977) on precipitation anomaly and
temperature delta. TPS has been widely used in climate science (Hijmans, Cameron, Parra, Jones, & Jarvis, 2005; Navarro-
Racines et al., 2020) as it produced a smooth and continuous surface, which is infinitely differentiable. Last, we multiplied the
change factor or added the delta to the WorldClim (1970-2000) data to get downscaled present-day monthly climate data.

Our future Köppen-Geiger map series are based on an ensemble of maps derived from the CCAFS bias-corrected and
170 downscaled climate projections, which include 35 CMIP5 GCMs, and 4 RCPs (Navarro-Racines et al., 2020). Large
misclassifications exist within the GCMs as detected in previous assessment of large areas ranging between 20-50% of the
total land area (Cui, Liang, & Wang, 2021). Deficiencies in model physics are also more likely to contribute to uncertainties
in the maps than grid size or reference dataset limitations (Tapiador, Moreno, & Navarro, 2019). Multi-model mean and delta-
change method can mitigate the bias effects from the threshold-based classification scheme and have been utilized to simulate
175 better results of climate classification (Hanf, Körper, Spanghel, & Cubasch, 2012). Therefore, we chose the CCAFS bias-
corrected and downscaled CMIP5 projections (Navarro-Racines et al., 2020) to reduce the amplified errors due to uncertainty
of climate projections. Navarro-Racines et al. (2020) interpolated anomalies of original GCM outputs using thin plate spline
spatial interpolation to achieve a baseline climate with a 1km surface. Then they applied delta method to the interpolated
baseline climates to correct the model biases (Hay, Wilby, & Leavesley, 2000; Ho, Stephenson, Collins, Ferro, & Brown,
180 2012).



3.3 Data Integration

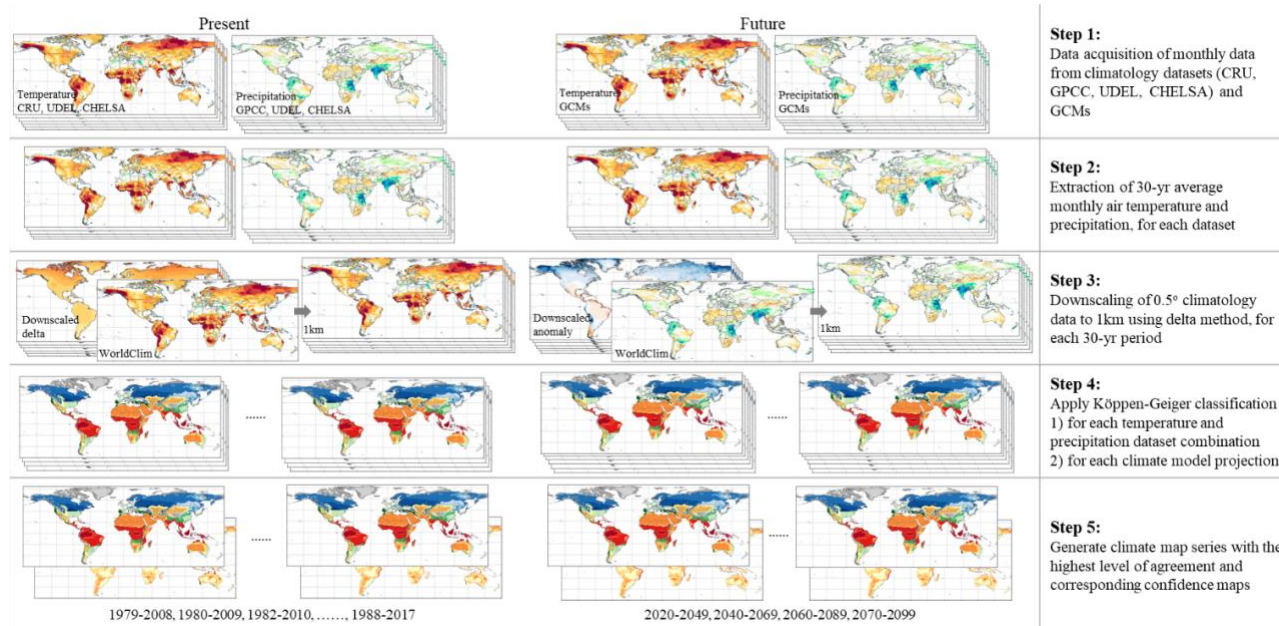


Figure 2. Step by step process to generate Köppen-Geiger climate map series.

The historical Köppen-Geiger climate classification map series was generated using the highest confidence class from an ensemble of maps using all combinations of surface air temperature and precipitation products (Fig. 2), as described in Beck et al. (2018). The highest confidence was given to the most common climate class for each grid cell. The final historical climate map series were derived using the climate class with the highest level of confidence in an ensemble of $3 \times 3 = 9$ classification maps based on combinations of the 3 precipitation datasets (CRU, UDEL, and CHELSA) and 3 surface air temperature datasets (GPCC, UDEL, and CHELSA). To further test the sensitivity of the method using the climate with the highest level of agreement, we incorporated another data integration method using the mean of multiple datasets. We quantified the degree of confidence placed in the Köppen-Geiger climate map series using the degree of confidence at the grid cell level calculated by dividing the occurrence frequency of the climate class with the highest level of agreement by the ensemble size. The calculated confidence level can be viewed as the agreement degree in classification resulted derived from different climatology datasets.

The future Köppen-Geiger climate classification map series under 4 RCPs, were derived based on the most common climate class from an ensemble of future climate maps. We generated a future Köppen-Geiger climate classification map for each climate model projection, using the CCAFS bias-corrected and downscaled CMIP5 GCM dataset. For example, the future Köppen-Geiger climate classification map series under RCP8.5 was derived from an ensemble of 30 maps based on 30 CMIP5 models. The level of confidence was estimated using the ratio between the frequency of the climate class with the highest level of agreement in the future map results, and the ensemble size.



200 **4 Results and Discussion**

4.1 Historical Köppen-Geiger climate maps

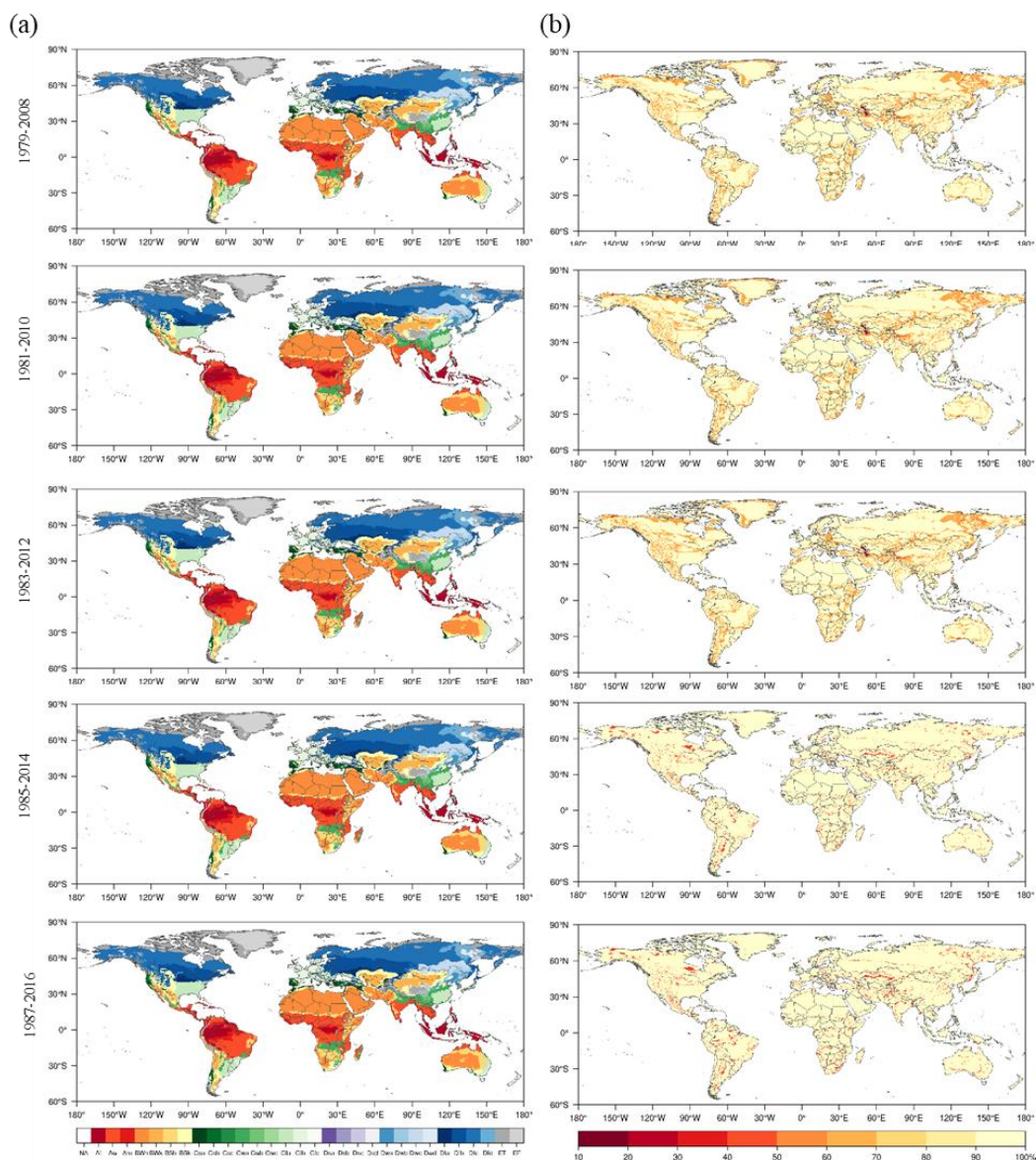


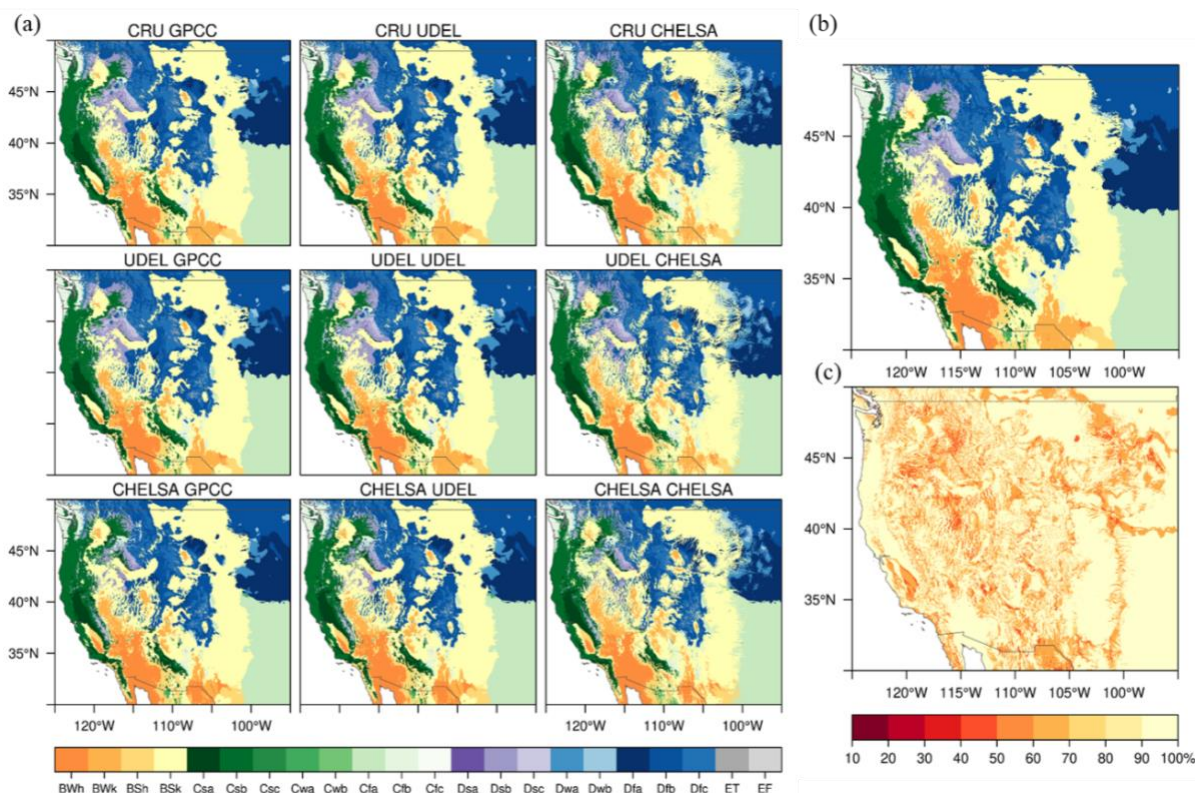
Figure 3 Global maps of Köppen-Geiger climate classification for the historical periods (1979-2008, 1981-2010, 1983-2012, 1985-2014, 1987-2016) and associated classification confidence levels. (a) Historical maps of Köppen-Geiger climate classification and (b) confidence levels associated with the Köppen-Geiger climate classification.

205

Global map series of Köppen-Geiger climate classification for historical periods and associated corresponding confidence levels are shown in Figure 3. Based on the distribution of confidence level, over 90% of the land area exhibit high level of confidence as classification results based on different climate data show excellent agreement. Relatively lower classification



accuracy and large discrepancy in classification results are found especially in mountainous regions such as Andes Mountains, Rocky Mountains, Tibetan Plateau, and major climate transitional zones located in mid and high latitudes of Northern Hemisphere, Central Africa, and Central Asia.



215 **Figure 4. Present Köppen-Geiger classification and confidence map for 1979-2008 with resolution of 1km for the central Rocky Mountains in North America.** (a) Climate maps based on the 9 combinations of the 3 precipitation datasets × 3 surface air temperature datasets, (b) the final climate map derived from the most common climate class among the 9 climate maps, and (c) confidence level distribution of the final climate map.

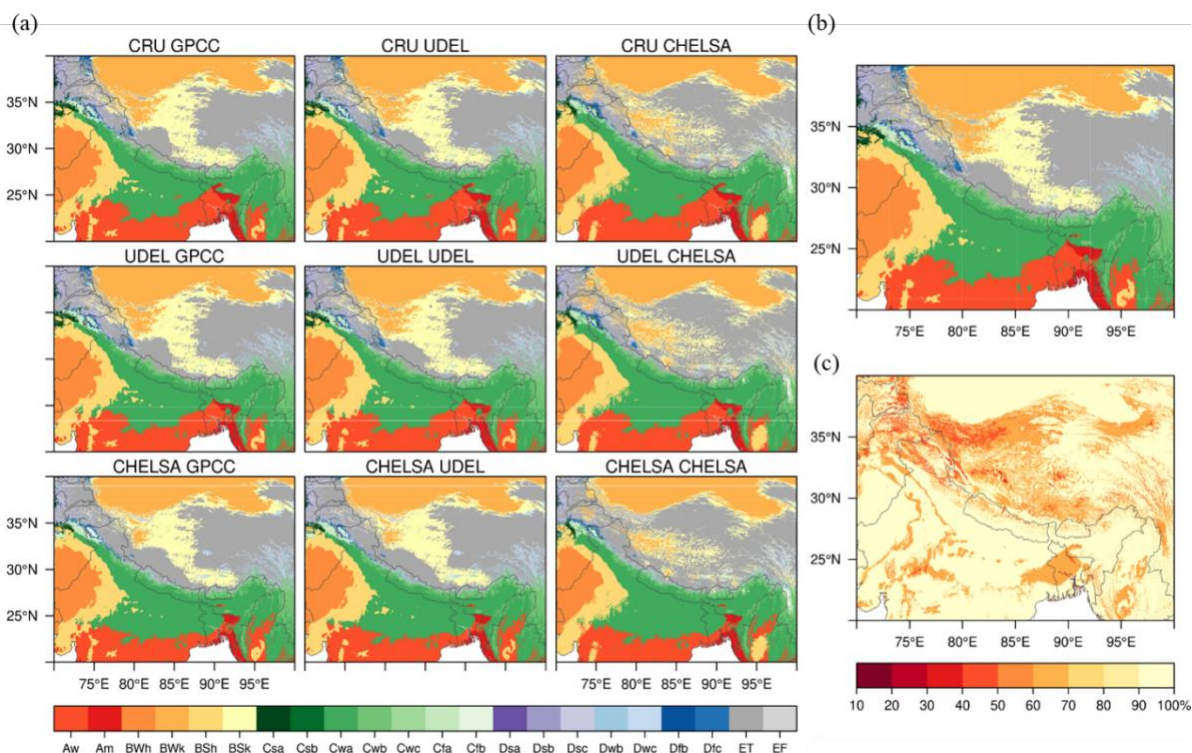


Figure 5. Present Köppen-Geiger classification and confidence map for 1979-2008 with resolution of 1km for the Tibetan Plateau.

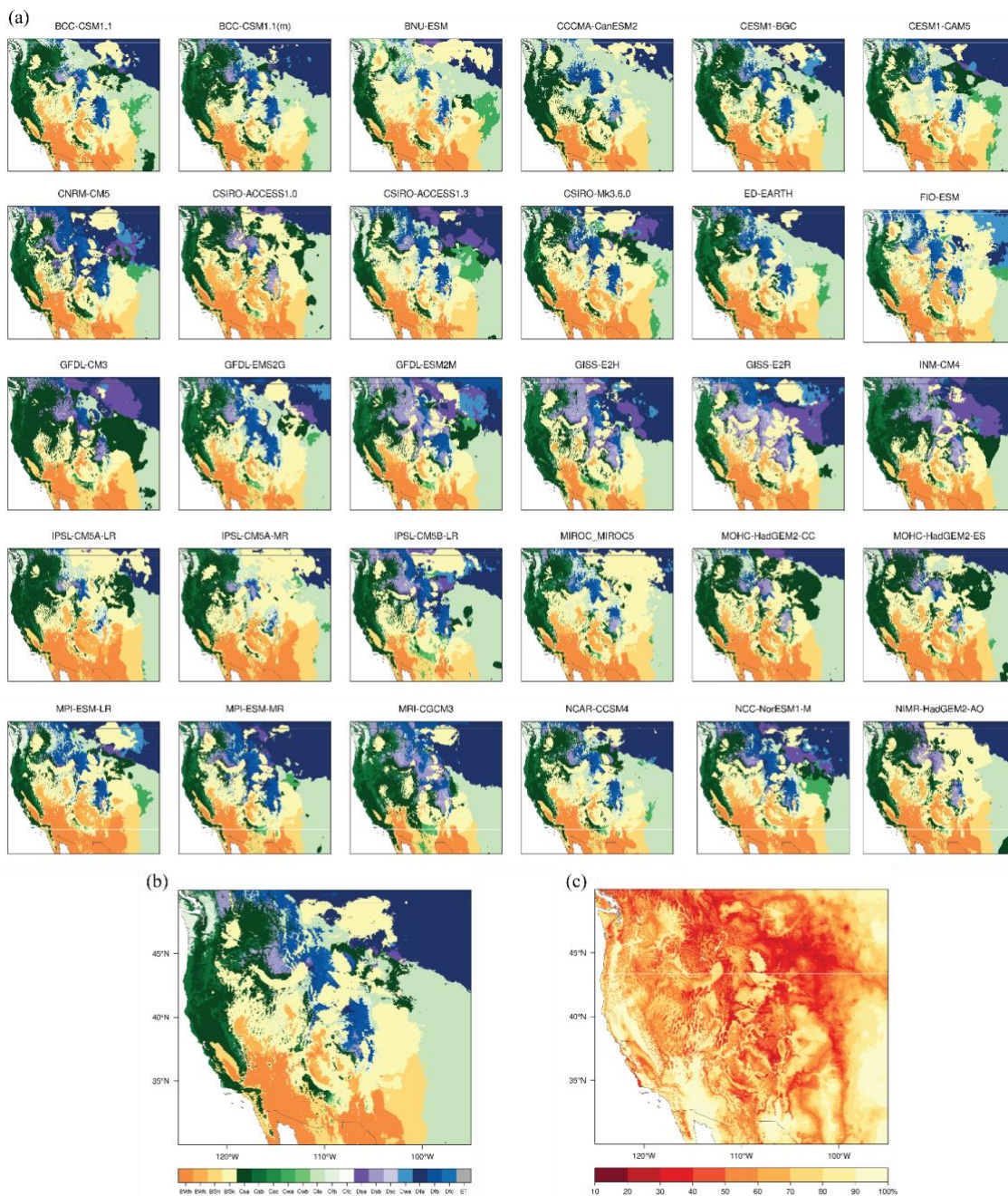
220

(a) Climate maps based on the 9 combinations of the 3 precipitation datasets \times 3 surface air temperature datasets, (b) the final climate map derived from the most common climate class among the 9 climate maps, and (c) confidence level distribution of the final climate map.

225

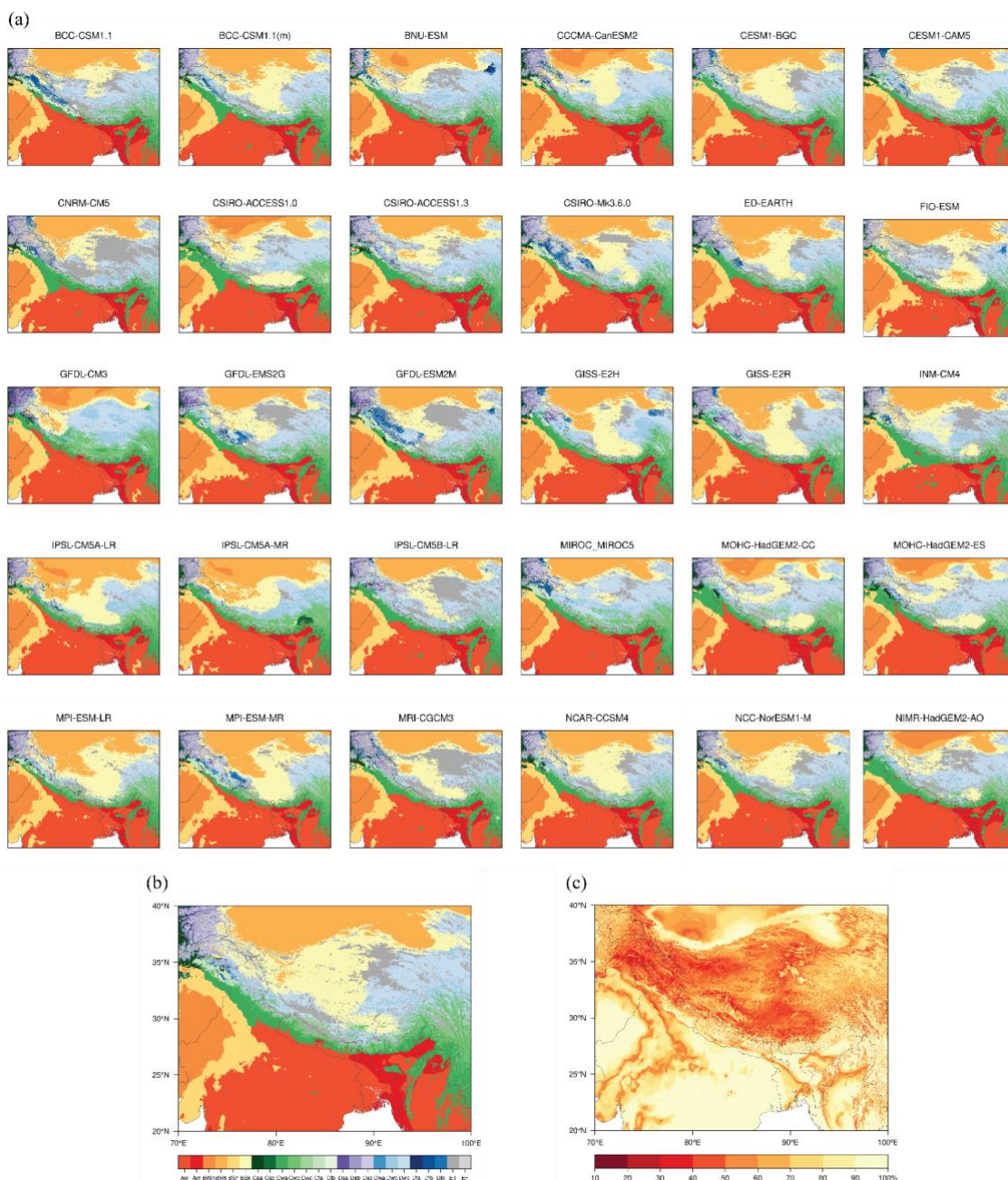
Regional distributions of climatic conditions are largely created by local variation in topography in rugged terrain (Dobrowski et al., 2013; Franklin et al., 2013). The climate classification and confidence level maps of mountainous areas of Central Rocky Mountains and Tibetan Plateau are shown in Figure 4 and 5 respectively. For each combination of precipitation and surface air temperature datasets, we generated a Köppen-Geiger climate classification map (see Fig. 4a and 5a for 1979-2008 maps for the central Rocky Mountains and Tibetan Plateau). The final Köppen-Geiger classification map is derived based on the most common climate type among all the climate maps (Fig. 4b and 5b). We then calculated corresponding confidence levels to quantify the uncertainty in the classification maps (Fig. 4c and 5c). The uncertainty in climate classification in mountainous areas is attributed to the uncertainty existing in climate data, especially precipitation data. In rugged terrain, CHELSA precipitation data shows more detailed precipitation patterns, causing disagreement in classification results of the 3rd level climate classes which depict precipitation seasonality.

230



240

Figure 7. Future Köppen-Geiger classification and confidence map for 2070-2099 under RCP8.5 with resolution of 1km for the central Rocky Mountains in North America. (a) Climate maps based on 30 GCMs, (b) the final climate map derived from the most common climate class among all the 30 climate maps, and (c) confidence level distribution of the final climate map.



245 **Figure 8. Future Köppen-Geiger classification and confidence map for 2070-2099 under RCP8.5 with resolution of 1km for the Tibetan Plateau.** (a) Climate maps based on 30 GCMs, (b) the final climate map derived from the most common climate class among all the 30 climate maps, and (c) confidence level distribution of the final climate map.

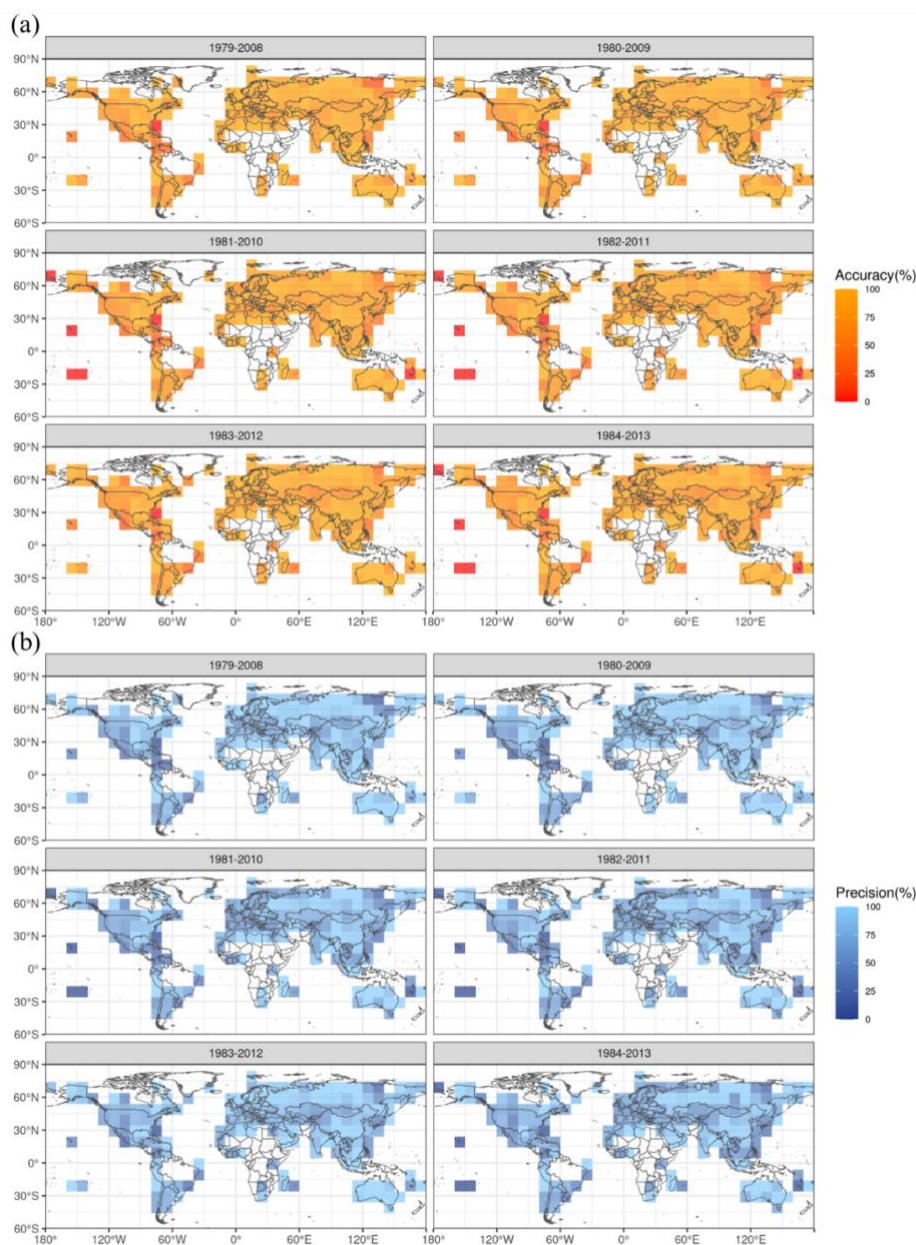
Future climate classifications derived from the diverse GCM projections for four RCPs, which are inherently uncertain (Gleckler, Taylor, & Doutriaux, 2008; Winsberg, 2012), provide a proxy of global distributions of climatic conditions and can



250 represent potential spatial changes in climate zones under global warming. The large uncertainty and strong disagreement in
projected climate classification maps at high latitudes and in regions with rugged terrain can be indicated by relatively low
confidence levels. Figure 7 and 8 show the future Köppen-Geiger climate classification maps based on GCM projections under
RCP8.5 and associated confidence levels for the central Rocky Mountains and Tibetan Plateau. We generated a future Köppen-
Geiger climate classification map for each bias-corrected and downscaled CMIP5 GCM projection (see Fig. 7a and 8a for
255 2070-2099 maps for the central Rocky Mountains and Tibetan Plateau). Noticeable regional changes in climate zones have
been projected by comparing the 2070-2099 and 1979-2008 climate classification maps (see Fig. 4b and 7b for the central
Rocky Mountains, and Fig. 5b and 8b for Tibetan Plateau).



4.3 Validation



260 **Figure 9. Validation of the historical Köppen-Geiger climate map series (1979-2008, 1980-2009, 1981-2010, 1982-2011, 1983-2012, 1984-2013).** (a) Small-scale accuracy of historical Köppen-Geiger climate maps. (b) Small-scale precision of historical Köppen-Geiger climate maps. Climate classification has been applied for each station. The small-scale accuracy and precision are calculated based on the classification results of all the stations within the given region, with a minimum of 3 stations in the 5° search radius.



265 We validated the historical climate maps using the station observations from Global Historical Climatology Network-Daily (GHCN-D) (Menne et al., 2012) and Global Summary Of the Day (GSOD) database (National Climatic Data Center et al., 2015) as reference data. For each station, time series of monthly temperature and precipitation were calculated from the daily observations with months with <15 daily values discarded. Then if ≥ 6 months are present, monthly climatology were generated subsequently by averaging the monthly means for the given period, typically 30 years. We discarded stations with

270 gap years or missing data in the given 30 years. For each station and each 30-yr period, we applied Köppen-Geiger climate classification. We evaluated overall classification performance for each climate map using total accuracy, which is defined as the percentage of correct classes, and average precision, which is averaged fraction of correct classification for all climate classes. Figure 9 shows the small-scale distributions of total accuracy and average precision for historical Köppen-Geiger climate map series with 10° grid cells. Due to uneven distributions of weather stations, remote areas in the Pacific islands,

275 Central Africa, and Amazon Forest suffer from a lack of station observations or an underrepresented validation results. Overall, the spatial patterns of total accuracy and average precision show good correspondence with classification confidence levels, indicating a potential of confidence level to represent classification uncertainty.

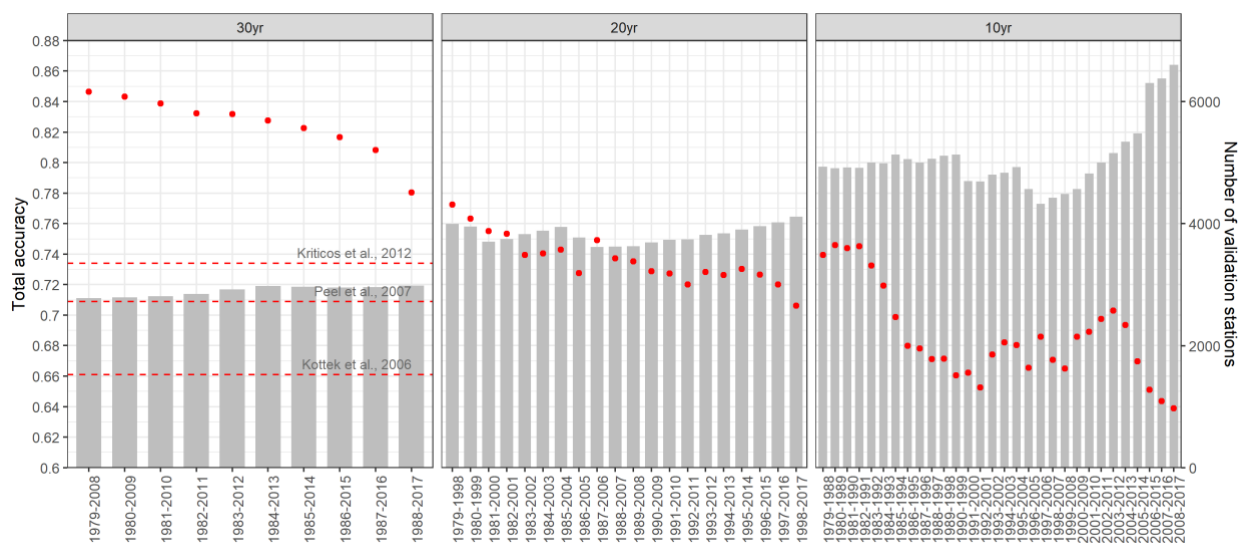
4.4 Sensitivity analysis

Table 3 Accuracy of the 1km Köppen-Geiger climate map series derived from different combinations of temperature and precipitation dataset input, and by different means of integration of multiple datasets. The values represent overall accuracy based on the technical validation using ground observation as reference.

Temperature Precipitation	CHELSA, Downscaled CRU and UDEL		Downscaled CRU and UDEL		CHELSA CHELSA
	CHELSA, Downscaled GPCP and UDEL		Downscaled GPCP and UDEL		
Integration of multiple datasets	Highest level of agreement	Mean of multiple datasets	Highest level of agreement	Mean of multiple datasets	-
1979-2008	83.25%	83.66%	83.13%	83.33%	79.72%
1980-2009	82.96%	83.44%	82.74%	82.78%	79.14%
1981-2010	82.63%	82.86%	81.95%	82.38%	78.03%
1982-2011	82.42%	82.73%	81.93%	82.11%	78.47%
1983-2012	81.48%	82.34%	81.14%	81.49%	78.32%
1984-2013	81.62%	82.05%	80.84%	81.27%	78.26%
1985-2014	-	-	80.23%	80.86%	-
1986-2015	-	-	79.79%	80.58%	-
1987-2016	-	-	78.76%	79.62%	-
1988-2017	-	-	-	78.65%	-
Average	82.39%	82.85%	81.17%	81.31%	78.66%
1980-2017 (Beck et al. 2018)	77.65%				



280 We tested sensitivity of the climate map series using different combinations of temperature and precipitation dataset, and different method of data integration (Table 3). Results indicated an average total accuracy of the 1km Köppen-Geiger classification maps generated with all the CHELSA, downscaled CRU, GPCC and UDEL datasets and with only downscaled CRU, GPCC, UDEL datasets as 82.39% and 81.17% respectively. Using the mean of multiple datasets which can potentially reduce the data bias, led to better classification results. Compared with the recently published Köppen-Geiger climate map product, Beck et al. (2018), the newly generated Köppen-Geiger climate map series showed greater accuracy in total.



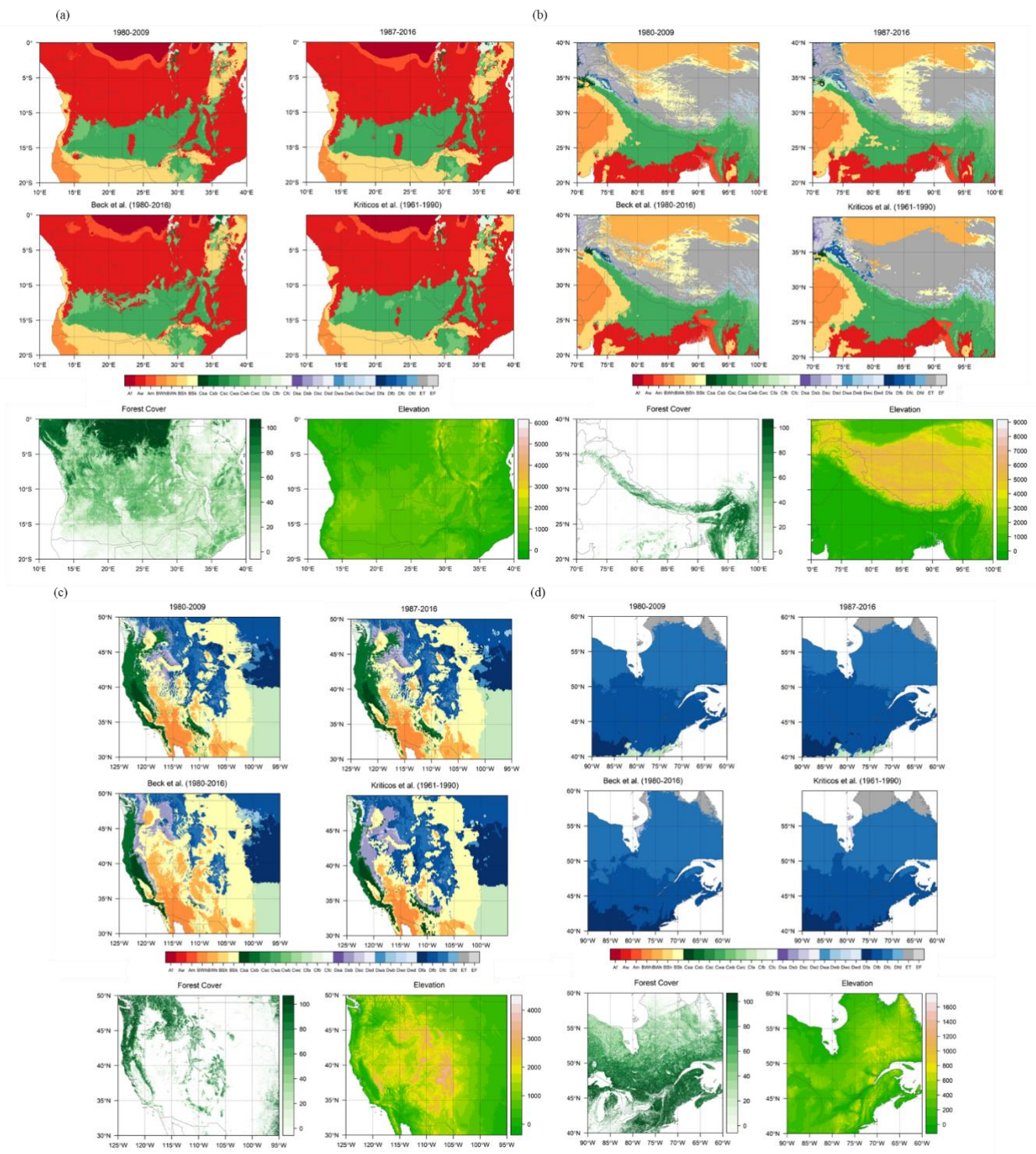
285

Figure 10. Validation of downscaled data of bioclimatic variables and the generated Köppen-Geiger climate map.

We conducted sensitivity analysis of the Köppen classification scheme and tested multiple time scales, 10-yr, 20-yr, and 30-yr. The selection criteria of station observations were adjusted accordingly based on the time scale utilized. Duplicate stations in the two datasets were further removed. Accuracy results exhibited decreasing accuracy for shorter time scale (Fig. 290 10). Further, we estimated the total accuracy for Köppen-Geiger climate classification maps from previous studies, Beck et al., (2018) Kriticos et al., (2012), Peel et al., (2007), and Kottek et al., (2006), using the same validation dataset and consistent Köppen-Geiger climate classification scheme the corresponding study applied. The validation results demonstrate that the new Köppen-Geiger maps have comparatively higher overall accuracy than all the previous studies.



4.5 Regional and continental scale comparison



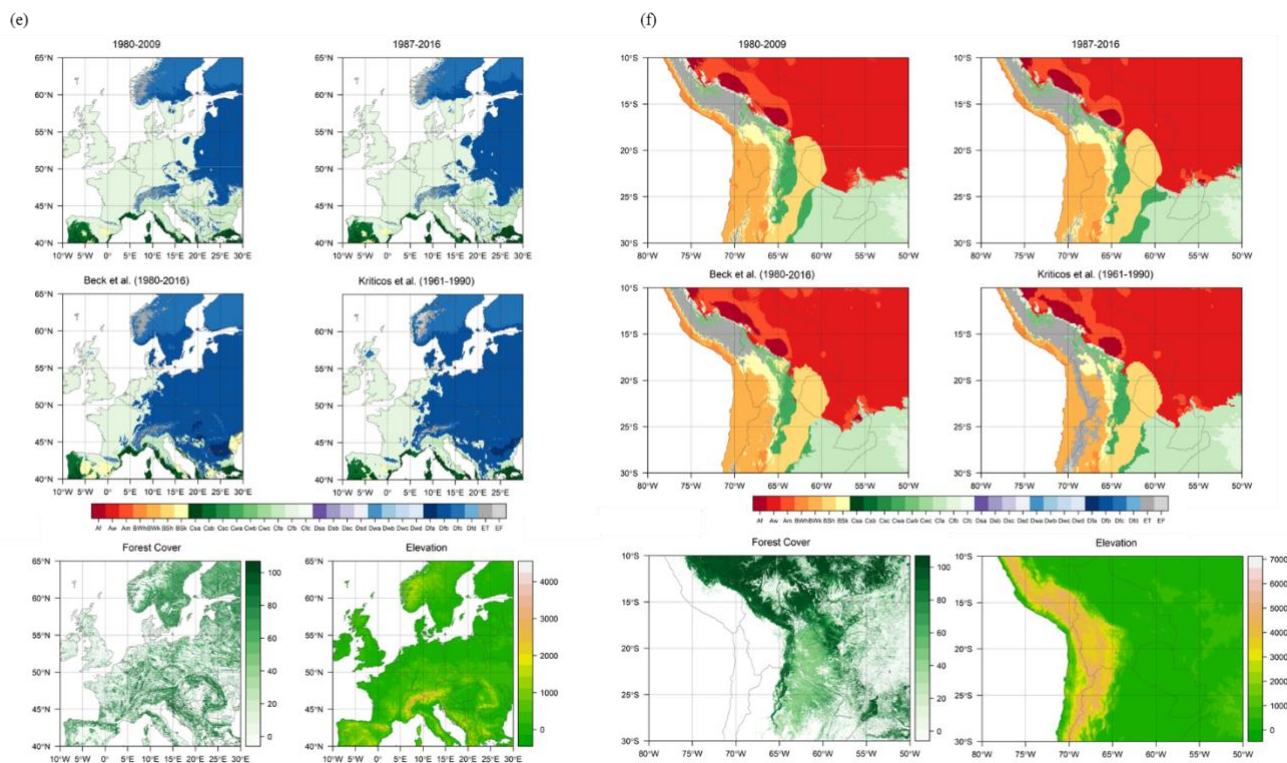


Figure 11. Köppen-Geiger climate classification maps from our study and previous studies, Beck et al., 2018, and Kriticos et al., 2012, associated forest cover and elevation maps, for regions with large spatial gradients in climates or sharp elevation gradients. (a) Central and eastern Africa, (b) Tibetan Plateau, (c) central Rocky Mountains, (d) high latitudes in North America, (e) Europe, and (f) central Andes. The forest cover map is the 30m Landsat-based forest cover map for year 2000 (Hansen et al., 2013). The elevation data is the NASA SRTM Digital Elevation 30m data (Farr et al., 2007). The representative period of each map is listed in parentheses.

300

At the regional and continental scale, we compared our Köppen-Geiger climate classification maps with previous map products for regions with large spatial gradients in climates, including central and eastern Africa, Europe, North America, and regions with sharp elevation gradients, including Tibetan Plateau, central Rocky Mountains, central Andes. The high-resolution Köppen-Geiger maps from two previous studies, Beck et al., (2018), and Kriticos et al., (2012) are used to evaluate the new Köppen-Geiger climate classification maps. To show the agreement between the improved Köppen-Geiger climate classification maps and regional landscape distributions, we showed maps of forest cover, and elevation distribution for these regions. The forest cover map we used is the 2000 30m Landsat-based forest cover map (Hansen et al., 2013). The elevation is from the NASA SRTM Digital Elevation 30m data (Farr et al., 2007). Figure 11 illustrate the enhanced regional details of the maps.

305

310

Compared with Köppen-Geiger climate maps from previous studies, the series of Köppen-Geiger climate maps from our study demonstrate the ability to capture recent changes in spatial distributions of climate zones. For example, our maps can detect



the significant changes in the arid (B) and polar (E) climate zones specifically driven by the accelerated global warming since
315 the 1980s (Cui, Liang, & Wang, 2021). Another improvement of the new series of Köppen-Geiger climate maps is the
application of threshold of -3 °C as the boundary of temperate (C) and boreal (D) climate zones, which show better agreement
with global boreal forest distributions compared with Russell's modification of 0 °C (1931), which Beck et al., (2018), and
Kriticos et al., (2012) utilized. Moreover, the new Köppen-Geiger maps show accurate depiction of important topographic
features and correspond closely with tree lines in the forest cover maps over the regions with complex topography (Fig. 11).

320 4.6 Bioclimatic variables

Table 4 List of bioclimatic variables derived from downscaled monthly climate data.

Bioclimatic Variables	Description
BIO1	Annual mean temperature (°C)
BIO2	Temperature of the warmest month (°C)
BIO3	Temperature of the coldest month (°C)
BIO4	Annual precipitation (mm)
BIO5	Precipitation of the warmest half year (mm)
BIO6	Precipitation of the coldest half year (mm)
BIO7	Precipitation of the driest month (mm)
BIO8	Precipitation of the driest month in the warmest half year (mm)
BIO9	Precipitation of the driest month in the coldest half year (mm)
BIO10	Precipitation of the wettest month (mm)
BIO11	Precipitation of the wettest month in the warmest half year (mm)
BIO12	Precipitation of the wettest month in the coldest half year (mm)

Beyond the Köppen-Geiger climate classification maps, we calculated a set of bioclimatic variables from the monthly climate
data (see full list in Table 4). The bioclimatic variables at 1-km spatial resolution can capture regional environmental variations
especially in mountainous areas and areas with strong climate variations. These bioclimatic variables can be used in studies
of environmental, agricultural and biological sciences, for example, development of species distribution modeling and
325 assessment of biological impacts induced by climate change. The variables provide descriptions of annual averages, and
seasonality of climates. The warmest half year or the coldest half year is defined as the period of the warmest six months or
the coldest six months.

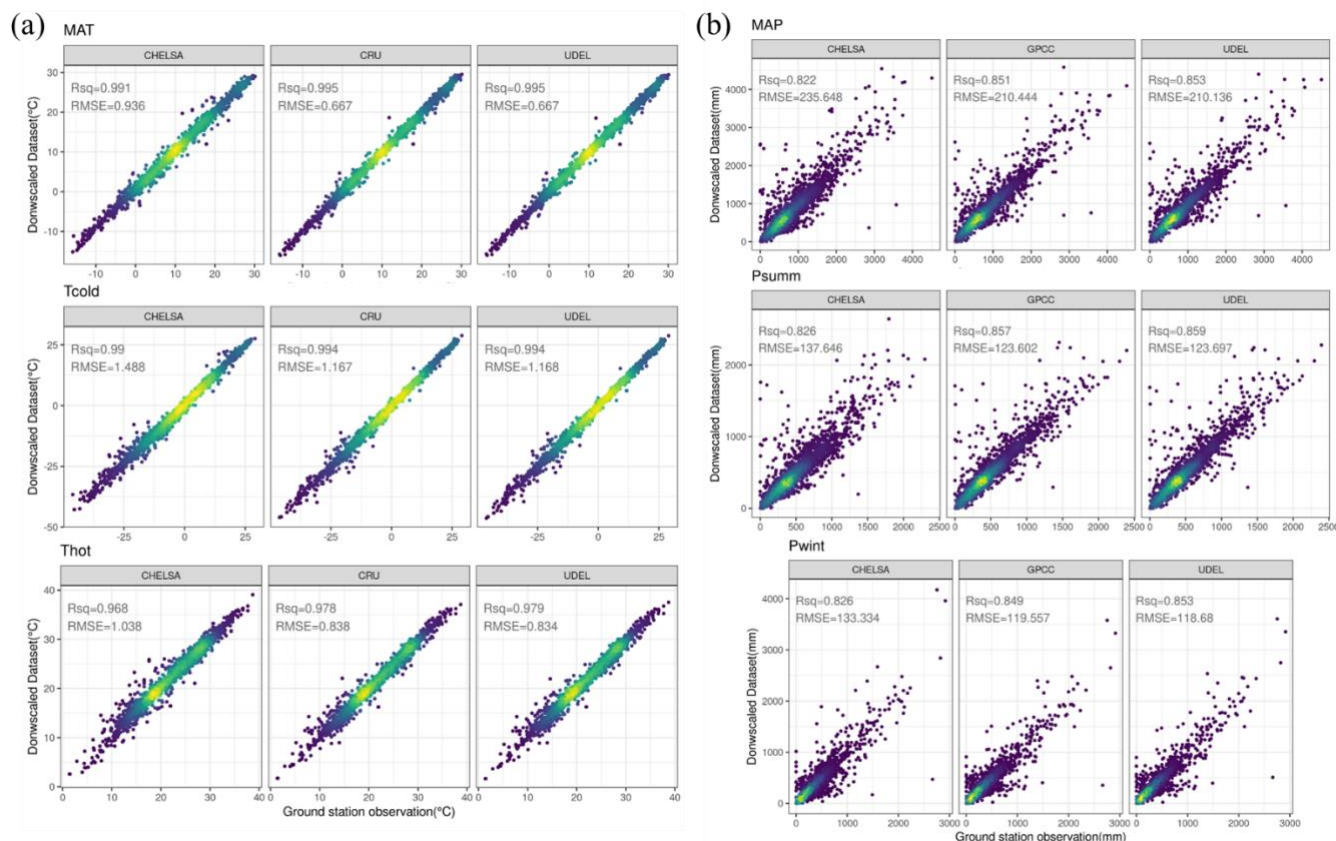
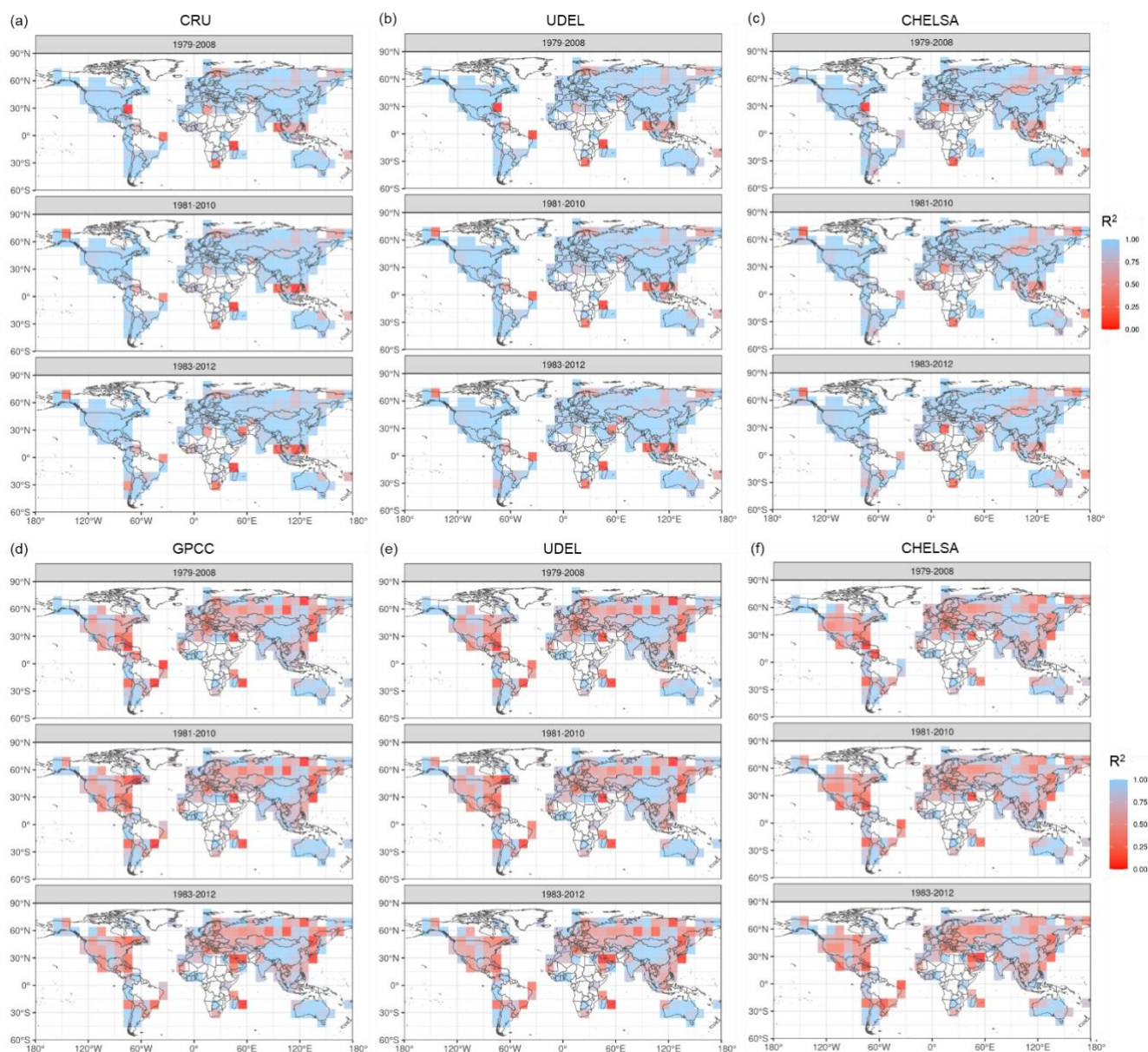


Figure 12. Scatter plots of the station observations and estimates of bioclimatic variables from downscaled climatology data. The bioclimatic variables include the 30-yr means of annual temperature (MAT), the air temperature of the coldest month (Tcold), the air temperature of the warmest month (Thot), total annual precipitation (MAP), precipitation of the summer half year (Psumm), and precipitation of the winter half year (Pwint). (a) Scatter plots of the station observations and downscaled temperature data from CHELSA, CRU, UDEL datasets, and (b) and downscaled precipitation data from CHELSA, GPCC, UDEL datasets.

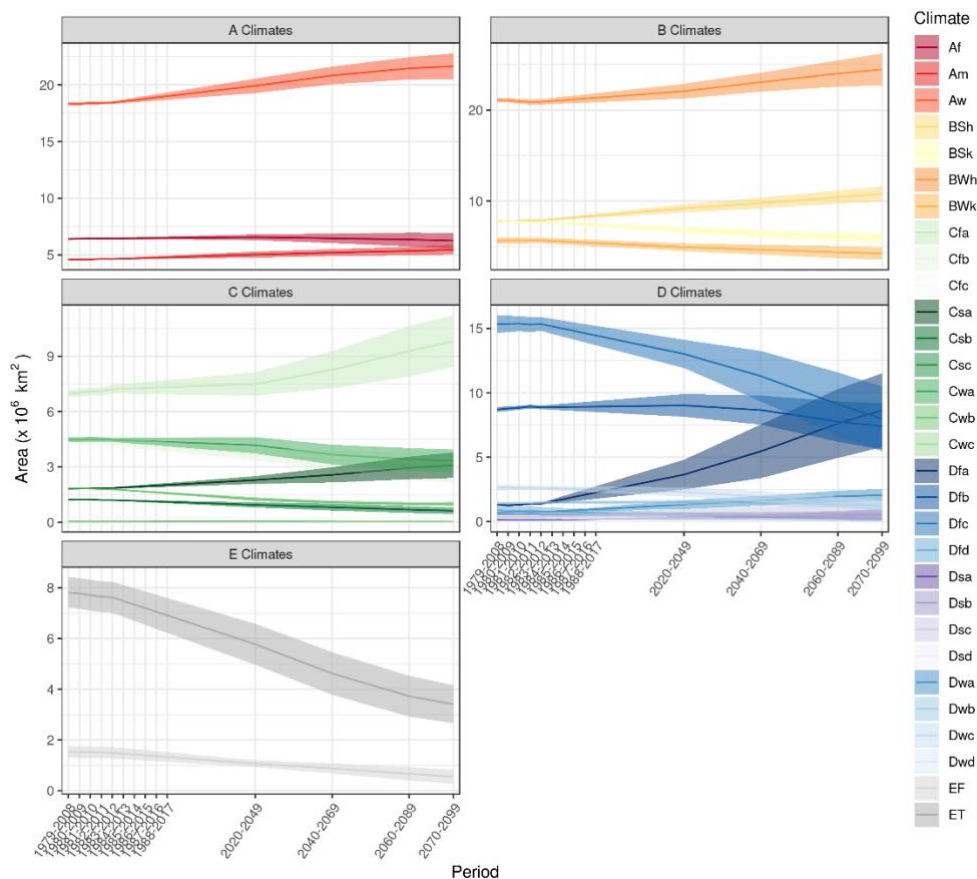
We validated the bioclimatic variables from different datasets with station data from GHCN-D (Menne et al., 2012) and GSOD database (National Climatic Data Center et al., 2015) (Fig. 12). We calculated a linear regression model for the 12 bioclimatic variables for each 10° grid cell (Fig. 13). The 30-yr average mean annual temperature (MAT) from CHELSA dataset shows overall highest fit with station data, with CRU, and UDEL datasets showing smaller, but still strong correlation with station data. The 30-yr average mean annual precipitation (MAP) estimates from GPCC, UDEL, and CHELSA datasets have considerable uncertainties, indicated by relatively low correlation with station observations. In current precipitation datasets, there exist a varied degree of discrepancy in annual estimates over multiple time scales (Sun et al., 2018).



345 **Figure 13. Small-scale comparison of annual temperature (MAT) and mean annual precipitation (MAP) variables derived from different datasets with station data.** Small-scale correlation between the 30-yr average mean annual temperature (MAT) and mean annual precipitation (MAP) data and ground observations for three historical periods (1979-2008, 1981-2010, 1983-2012). The station data is from GHCN-D and GSOD database. The figure shows the R^2 value for 10° grid cells. (a), (b), and (c) are MAT results. (d), (e), and (f) are MAP results. (a) MAT is calculated from downscaled monthly temperature data from CRU dataset, (b) from UDEL dataset and (c) from CHELSA dataset. (d) MAP is calculated from downscaled monthly precipitation data from GPCP dataset, (e) from UDEL dataset and (f) from CHELSA dataset.



350 **4.7 Application example: detection of area changes in climate zones**



355 **Figure 14. Area changes in climate zones since the 1980s on a global scale under RCP8.5.** The error bars for historical periods (1979-2017) indicate standard error in the Köppen-Geiger classification results based on the 9 combinations of observational air temperature and precipitation datasets and for future periods (2020-2099), the error bars indicate standard error in the Köppen-Geiger classification results based on the 30 GCMs.

Changes in climatic conditions under global warming have significant impacts on biodiversity and ecological systems. Area changes of climate zones can indicate spatial shrinkage or expansion of analogous climatic conditions, potentially implying threats for species range contraction or opportunities for range expansion (Cui, Liang, & Wang, 2021). To examine the area changes of climate zones, we calculated the total area covered by each climate type for each historical and future periods under high-emission RCP8.5 scenario (Fig. 14). Our results of changes in area occupied by different climate zones demonstrate good agreement with results from previous studies (Chan & Wu, 2015). Results show that accelerated anthropogenic global warming since the 1980s has caused large-scale changes in climate zones and the shifts into warmer and drier climates are projected in this century. The tropical and arid climates are expanding into large areas in mid latitudes whereas the high-latitude climates will experience significant area shrinkage.



365 5 Conclusion

Changes in broad-scale climatic conditions, driven by anthropogenic global warming, lead to the redistribution of species diversity and the reorganization of ecosystems. Distributions of the Earth's climatic conditions have been widely characterized based on the Köppen climate classification system. Köppen climate classification maps require fine resolutions of at least 1-km to detect relevant microrefugia and promote effective conservation. Studies examining recent and future interannual or
370 interdecadal changes in climate zones at regional scale needs more accurate depiction of fine-grained climatic conditions, continuous and longer temporal coverage.

We presented an improved long-term Köppen-Geiger climate classification map series for ten historical 30-yr periods in 1979-2017 and four future 30-yr periods in 2020-2099 under RCP2.6, 4.5, 6.0 and 8.5. To improve the classification accuracy and achieve a resolution as fine as 1-km, we combined multiple datasets, including WorldClim V2, CHELSA V1.2, CRU TS v4.03,
375 UDEL, GPCC datasets and bias-corrected downscaled CMIP5 model simulations from CCAFS. The historical climate maps are based on the most common climate type from an ensemble of climate maps derived from combinations of observational climatology datasets. The future climate maps are based on an ensemble of climate maps derived from 35 GCMs. We estimated the corresponding confidence levels to quantify the uncertainty in climate maps. We also calculated 12 bioclimatic variables at the same 1-km resolution using these climate datasets for the same historical and future periods to provide data of annual
380 averages, seasonality, and stressful conditions of climates.

To validate the Köppen-Geiger climate classification maps, we used the station observations from GHCN-D and GSOD database. Our validation results show that the new Köppen-Geiger maps have comparatively higher overall accuracy than all the previous studies. Although the new maps exhibit improved overall accuracy, relatively lower confidence level and larger discrepancy in classification results are found especially in mountainous regions and major climate transitional zones located
385 in mid and high latitudes. The confidence levels can provide a useful quantification of classification uncertainty.

Compared with climate maps from previous studies with a single present-day period, the series of Köppen-Geiger climate maps from our study demonstrate the ability to capture recent and future projected changes in spatial distributions of climate zones. On regional and continental scale, the new maps show accurate depictions of topographic features and correspond closely with vegetation distributions. Our Köppen-Geiger climate classification maps can offer a descriptive and ecological
390 relevant way to provide insights into changes in spatial distributions of climate zones.

One of the limitations is that the future of Köppen-Geiger climate maps built on downscaled climate model projections exist unavoidable uncertainties. The classification agreement levels of GCMs are relatively low at high latitudes and in regions with rugged terrain. The main sources of model discrepancies and uncertainties are deficiencies in model physics and varied model resolution. The climate model outputs have coarse spatial resolution varying from 70-400 km and cannot well represent future
395 climate change at the same scale of 1-km as our baseline climatology. Through bias-correction and downscaling methods, we



made assumptions that local relationships between climatic variables remain constant across different scales, leading to a compromise between spatial scale and climate model physics.

We also tested the sensitivity of classification results to different time scale, dataset input, and data integration methods. Results show that 30-yr time scale exhibited the highest accuracy results. Moreover, using the mean of multiple datasets from CHELSA, CRU, UDEL, and GPCC could lead to better classification results. Last, we provided a heuristic example which used climate classification map series to detect the long-term area changes of climate zones, showing how the new Köppen-Geiger climate classification map series can be applied in climate change studies. With improved accuracy, high spatial resolution, long-term continuous time coverage, this global dataset of Köppen-Geiger climate classification and bioclimatic variables can be used to in conjunction with species distribution models to promote biodiversity conservation, and to analyse and identify recent and future interannual or interdecadal changes in climate zones on a global or regional scale.

Data Availability

This high-resolution global dataset of Köppen-Geiger climate classification and bioclimatic variables dataset for historical periods in 1979-2017 is available at <http://doi.org/10.5281/zenodo.4546140> (Cui, Liang, Wang, & Liu, 2021b). The dataset for future periods in 2020-2100 is available at <http://doi.org/10.5281/zenodo.4542076> (Cui, Liang, Wang, & Liu, 2021a).

410 Author Contribution

C.D. designed the computational framework, performed data collection and processing, conducted validation and sensitivity analyzes, and wrote the manuscript. L.Z. contributed to the data processing. L.S. was involved in planning and supervised the work. All authors discussed the results and commented on the manuscript.

Competing Interests

415 The authors declare that they have no conflict of interest.

References

- Beck, C., Grieser, J., & Rudolf, B. (2005). A new monthly precipitation climatology for the global land areas for the period 1951 to 2000. *Klimastatusbericht KSB, 2004*.
- Beck, H. E., Zimmermann, N. E., McVicar, T. R., Vergopolan, N., Berg, A., & Wood, E. F. (2018). Present and future Köppen-Geiger climate classification maps at 1-km resolution. *Scientific Data, 5*, 180214.
<https://doi.org/10.1038/sdata.2018.214>



- Belda, M., Holtanová, E., Halenka, T., & Kalvová, J. (2014). Climate classification revisited: From Köppen to Trewartha. *Climate Research*, 59(1), 1–13. <https://doi.org/10.3354/cr01204>
- Belda, M., Holtanová, E., Kalvová, J., & Halenka, T. (2016). Global warming-induced changes in climate zones based on
425 CMIP5 projections. *Climate Research*, 71(1), 17–31. <https://doi.org/10.3354/cr01418>
- Bockheim, J. G., Gennadiyev, A. N., Hammer, R. D., & Tandarich, J. P. (2005). Historical development of key concepts in pedology. *Geoderma*, 124(1-2), 23–36. <https://doi.org/10.1016/j.geoderma.2004.03.004>
- Booth, Trevor H., Henry A. Nix, John R. Busby, and Michael F. Hutchinson. “BIOCLIM: The First Species Distribution
430 Modelling Package, Its Early Applications and Relevance to Most Current MaxEnt Studies.” Edited by Janet Franklin. *Diversity and Distributions* 20, no. 1 (January 2014): 1–9. <https://doi.org/10.1111/ddi.12144>.
- Brugger, K., & Rubel, F. (2013). Characterizing the species composition of European *Culicoides* vectors by means of the Köppen-Geiger climate classification. *Parasites & Vectors*, 6(1), 333. <https://doi.org/10.1186/1756-3305-6-333>
- Chan, D., & Wu, Q. (2015). Significant anthropogenic-induced changes of climate classes since 1950. *Scientific Reports*, 5, 13487. <https://doi.org/10.1038/srep13487>
- 435 Chen, D., & Chen, H. W. (2013). Using the Köppen classification to quantify climate variation and change: An example for 1901–2010. *Environmental Development*, 6, 69–79. <https://doi.org/10.1016/j.envdev.2013.03.007>
- Chen, I.-C., Hill, J. K., Ohlemüller, R., Roy, D. B., & Thomas, C. D. (2011). Rapid range shifts of species associated with high levels of climate warming. *Science (New York, N.Y.)*, 333(6045), 1024–1026. <https://doi.org/10.1126/science.1206432>
- 440 Chen, M., Xie, P., Janowiak, J. E., & Arkin, P. A. (2002). Global land precipitation: A 50-yr monthly analysis based on gauge observations. *Journal of Hydrometeorology*, 3(3), 249–266.
- Craven, P., & Wahba, G. (1978). Smoothing noisy data with spline functions. *Numerische Mathematik*, 31(4), 377–403. <https://doi.org/10.1007/BF01404567>
- Cui, D., Liang, S., & Wang, D. (2021). Observed and projected changes in global climate zones based on Köppen climate
445 classification. *Wiley Interdisciplinary Reviews: Climate Change*, e701. <https://doi.org/10.1002/wcc.701>
- Cui, D., Liang, S., Wang, D., & Liu, Z. (2021a). KGClim future: A 1-km global dataset of future (2020–2100) Köppen-Geiger climate classification and bioclimatic variables (Version V1). Advance online publication. <https://doi.org/10.5281/zenodo.4542076>
- Cui, D., Liang, S., Wang, D., & Liu, Z. (2021b). KGClim historical: A 1-km global dataset of historical (1979–2017)
450 Köppen-Geiger climate classification and bioclimatic variables (Version V1). Advance online publication. <https://doi.org/10.5281/zenodo.4546140>



- Dobrowski, S. Z., Abatzoglou, J., Swanson, A. K., Greenberg, J. A., Mynsberge, A. R., Holden, Z. A., & Schwartz, M. K. (2013). The climate velocity of the contiguous United States during the 20th century. *Global Change Biology*, *19*(1), 241–251. <https://doi.org/10.1111/gcb.12026>
- 455 Fan, Y., & Dool, H. v. d. (2008). A global monthly land surface air temperature analysis for 1948–present. *Journal of Geophysical Research*, *113*(D1), 161. <https://doi.org/10.1029/2007JD008470>
- Farr, T. G., Rosen, P. A., Caro, E., Crippen, R., Duren, R., Hensley, S., . . . Alsdorf, D. (2007). The Shuttle Radar Topography Mission. *Reviews of Geophysics*, *45*(2), 1485. <https://doi.org/10.1029/2005RG000183>
- Feng, S., Ho, C.-H., Hu, Q., Oglesby, R. J., Jeong, S.-J., & Kim, B.-M. (2012). Evaluating observed and projected future
460 climate changes for the Arctic using the Köppen-Trewartha climate classification. *Climate Dynamics*, *38*(7-8), 1359–1373. <https://doi.org/10.1007/s00382-011-1020-6>
- Feng, S., Hu, Q., Huang, W., Ho, C.-H., Li, R., & Tang, Z. (2014). Projected climate regime shift under future global warming from multi-model, multi-scenario CMIP5 simulations. *Global and Planetary Change*, *112*, 41–52. <https://doi.org/10.1016/j.gloplacha.2013.11.002>
- 465 Fick, S. E., & Hijmans, R. J. (2017). WorldClim 2: New 1-km spatial resolution climate surfaces for global land areas. *International Journal of Climatology*, *37*(12), 4302–4315. <https://doi.org/10.1002/joc.5086>
- Franke, R. (1982). Smooth interpolation of scattered data by local thin plate splines. *Computers & Mathematics with Applications*, *8*(4), 273–281. [https://doi.org/10.1016/0898-1221\(82\)90009-8](https://doi.org/10.1016/0898-1221(82)90009-8)
- Franklin, J., Davis, F. W., Ikegami, M., Syphard, A. D., Flint, L. E., Flint, A. L., & Hannah, L. (2013). Modeling plant
470 species distributions under future climates: How fine scale do climate projections need to be? *Global Change Biology*, *19*(2), 473–483. <https://doi.org/10.1111/gcb.12051>
- Garcia, R. A., Cabeza, M., Rahbek, C., & Araújo, M. B. (2014). Multiple dimensions of climate change and their implications for biodiversity. *Science (New York, N.Y.)*, *344*(6183), 1247579. <https://doi.org/10.1126/science.1247579>
- Geiger, R. (1961). bearbeitete Neuauflage von Geiger, R.: Köppen-Geiger/Klima der Erde. *Wandkarte (wall map)*, *1*, 16.
- 475 Gleckler, P. J., Taylor, K. E., & Doutriaux, C. (2008). Performance metrics for climate models. *Journal of Geophysical Research*, *113*(D6), 1147. <https://doi.org/10.1029/2007JD008972>
- Grieser, J., Gommel, R., Cofield, S., & Bernardi, M. (2006). New gridded maps of Koeppen’s climate classification.
- Hanf, F., Körper, J., Spangehl, T., & Cubasch, U. (2012). Shifts of climate zones in multi-model climate change experiments using the Köppen climate classification. *Meteorologische Zeitschrift*, *21*(2), 111–123. <https://doi.org/10.1127/0941-4802948/2012/0344>



- Hansen, M. C., Potapov, P. V., Moore, R., Hancher, M., Turubanova, S. A., Tyukavina, A., . . . Townshend, J. R. G. (2013). High-resolution global maps of 21st-century forest cover change. *Science (New York, N.Y.)*, 342(6160), 850–853. <https://doi.org/10.1126/science.1244693>
- 485 Hartmann, D. L., A.M.G. Klein Tank, M. Rusticucci, L.V. Alexander, S. Brönnimann, Y. Charabi, . . . P.M. Zhai (2013). *Observations: Atmosphere and Surface*. In: Climate Change 2013: The Physical Science Basis. Contribution of Working Group I to the Fifth Assessment Report of the Intergovernmental Panel on Climate Change [Stocker, T.F., D. Qin, G.-K. Plattner, M. Tignor, S.K. Allen, J. Boschung, A. Nauels, Y. Xia, V. Bex and P.M. Midgley (eds.)]. Cambridge, United Kingdom and New York, NY, USA: Cambridge University Press.
- 490 Hay, L. E., Wilby, R. L., & Leavesley, G. H. (2000). A comparison of delta change and downscaled GCM scenarios for three mountainous basins in the united states. *JAWRA Journal of the American Water Resources Association*, 36(2), 387–397. <https://doi.org/10.1111/j.1752-1688.2000.tb04276.x>
- Hijmans, R. J., Cameron, S. E., Parra, J. L., Jones, P. G., & Jarvis, A. (2005). Very high resolution interpolated climate surfaces for global land areas. *International Journal of Climatology*, 25(15), 1965–1978. <https://doi.org/10.1002/joc.1276>
- 495 Ho, C. K., Stephenson, D. B., Collins, M., Ferro, C. A. T., & Brown, S. J. (2012). Calibration strategies: A source of additional uncertainty in climate change projections. *Bulletin of the American Meteorological Society*, 93(1), 21–26. <https://doi.org/10.1175/2011BAMS3110.1>
- Holdridge, L. R. (1947). Determination of world plant formations from simple climatic data. *Science (New York, N.Y.)*, 105(2727), 367–368. <https://doi.org/10.1126/science.105.2727.367>
- Jones, S. B. (1932). Classifications of North American climates: A review. *Economic Geography*, 8(2), 205–208. <https://doi.org/10.2307/140250>
- 500 Karger, D. N., Conrad, O., Böhner, J., Kawohl, T., Kreft, H., Soria-Auza, R. W., . . . Kessler, M. (2017). Climatologies at high resolution for the earth's land surface areas. *Scientific Data*, 4, 170122. <https://doi.org/10.1038/sdata.2017.122>
- Köppen, W. (1900). Versuch einer Klassifikation der Klimate, vorzugsweise nach ihren Beziehungen zur Pflanzenwelt. *Geographische Zeitschrift*, 6(11), 593–611.
- 505 Köppen, W. (1884). Die Wärmezonen der Erde, nach der Dauer der heissen, gemässigten und kalten Zeit und nach der Wirkung der Wärme auf die organische Welt betrachtet. *Meteorologische Zeitschrift*, 1(21), 5–226.
- Köppen, W. P. (1931). Grundriss der klimakunde.
- Köppen, W. P. (1936). *Das geographische System der Klimate: Mit 14 Textfiguren*: Borntraeger.
- Kottek, M., Grieser, J., Beck, C., Rudolf, B., & Rubel, F. (2006). World map of the Köppen-Geiger climate classification updated. *Meteorologische Zeitschrift*, 15(3), 259–263. <https://doi.org/10.1127/0941-2948/2006/0130>
- 510



- Kriticos, D. J., Webber, B. L., Leriche, A., Ota, N., Macadam, I., Bathols, J., & Scott, J. K. (2012). CliMond: Global high-resolution historical and future scenario climate surfaces for bioclimatic modelling. *Methods in Ecology and Evolution*, 3(1), 53–64. <https://doi.org/10.1111/j.2041-210X.2011.00134.x>
- 515 Leemans, R., Cramer, W., & van Minnen, J. G. (1996). Prediction of global biome distribution using bioclimatic equilibrium models. *SCOPE-SCIENTIFIC COMMITTEE ON PROBLEMS OF THE ENVIRONMENT INTERNATIONAL COUNCIL OF SCIENTIFIC UNIONS*, 56, 413–440.
- Mahlstein, I., Daniel, J. S., & Solomon, S. (2013). Pace of shifts in climate regions increases with global temperature. *Nature Climate Change*, 3(8), 739–743. <https://doi.org/10.1038/nclimate1876>
- 520 Manabe, S., & Holloway, J. L. (1975). The seasonal variation of the hydrologic cycle as simulated by a global model of the atmosphere. *Journal of Geophysical Research*, 80(12), 1617–1649. <https://doi.org/10.1029/JC080i012p01617>
- Menne, M. J., Durre, I., Vose, R. S., Gleason, B. E., & Houston, T. G. (2012). An overview of the global historical climatology network-daily database. Advance online publication. <https://doi.org/10.1175/jtech-d-11-00103.1>
- National Climatic Data Center, NESDIS, NOAA, & U.S. Department of Commerce (2015). Global Surface Summary of the Day - GSOD. Retrieved from <https://data.nodc.noaa.gov/cgi-bin/iso?id=gov.noaa.ncdc:C00516#>
- 525 Navarro-Racines, C., Tarapues, J., Thornton, P., Jarvis, A., & Ramirez-Villegas, J. (2020). High-resolution and bias-corrected CMIP5 projections for climate change impact assessments. *Scientific Data*, 7(1), 7. <https://doi.org/10.1038/s41597-019-0343-8>
- Netzel, P., & Stepinski, T. (2016). On using a clustering approach for global climate classification. *Journal of Climate*, 29(9), 3387–3401. <https://doi.org/10.1175/JCLI-D-15-0640.1>
- 530 New, M., Hulme, M., & Jones, P. (2000). Representing twentieth-century space–time climate variability. Part II: Development of 1901–96 monthly grids of terrestrial surface climate. *Journal of Climate*, 13(13), 2217–2238. [https://doi.org/10.1175/1520-0442\(2000\)013<2217:RTCSTC>2.0.CO;2](https://doi.org/10.1175/1520-0442(2000)013<2217:RTCSTC>2.0.CO;2)
- Ordonez, A., & Williams, J. W. (2013). Projected climate reshuffling based on multivariate climate-availability, climate-analog, and climate-velocity analyses: Implications for community disaggregation. *Climatic Change*, 119(3-4), 659–675. <https://doi.org/10.1007/s10584-013-0752-1>
- 535 Peel, M. C., Finlayson, B. L., & McMahon, T. A. (2007). Updated world map of the Köppen-Geiger climate classification. *Hydrology and Earth System Sciences Discussions*, 4(2), 439–473. <https://doi.org/10.5194/hessd-4-439-2007>
- Peel, M. C., McMahon, T. A., Finlayson, B. L., & Watson, F. G.R. (2001). Identification and explanation of continental differences in the variability of annual runoff. *Journal of Hydrology*, 250(1-4), 224–240. [https://doi.org/10.1016/S0022-1694\(01\)00438-3](https://doi.org/10.1016/S0022-1694(01)00438-3)
- 540 Pinsky, M. L., Worm, B., Fogarty, M. J., Sarmiento, J. L., & Levin, S. A. (2013). Marine taxa track local climate velocities. *Science (New York, N.Y.)*, 341(6151), 1239–1242. <https://doi.org/10.1126/science.1239352>



- Poulter, B., Ciais, P., Hodson, E., Lischke, H., Maignan, F., Plummer, S., & Zimmermann, N. E. (2011). Plant functional type mapping for earth system models. *Geoscientific Model Development*, 4(4), 993–1010. <https://doi.org/10.5194/gmd-4-993-2011>
545
- Roderfeld, H., Blyth, E., Dankers, R., Huse, G., Slagstad, D., Ellingsen, I., . . . Lange, M. A. (2008). Potential impact of climate change on ecosystems of the Barents Sea Region. *Climatic Change*, 87(1-2), 283–303. <https://doi.org/10.1007/s10584-007-9350-4>
- Rohli, R. V., Andrew, J. T., Reynolds, S. J., Shaw, C., & Vázquez, J. R. (2015). Globally extended Köppen–Geiger climate classification and temporal shifts in terrestrial climatic types. *Physical Geography*, 36(2), 142–157. <https://doi.org/10.1080/02723646.2015.1016382>
550
- Rohli, R. V., Joyner, T. A., Reynolds, S. J., & Ballinger, T. J. (2015). Overlap of global Köppen–Geiger climates, biomes, and soil orders. *Physical Geography*, 36(2), 158–175. <https://doi.org/10.1080/02723646.2015.1016384>
- Rubel, F., Brugger, K., Haslinger, K., & Auer, I. (2017). The climate of the European Alps: Shift of very high resolution Köppen–Geiger climate zones 1800–2100. *Meteorologische Zeitschrift*, 26(2), 115–125. <https://doi.org/10.1127/metz/2016/0816>
555
- Rubel, F., & Kottek, M. (2010). Observed and projected climate shifts 1901–2100 depicted by world maps of the Köppen–Geiger climate classification. *Meteorologische Zeitschrift*, 19(2), 135–141. <https://doi.org/10.1127/0941-2948/2010/0430>
- Rubel, F., & Kottek, M. (2011). Comments on: "The thermal zones of the Earth" by Wladimir Köppen (1884). *Meteorologische Zeitschrift*, 20(3), 361–365. <https://doi.org/10.1127/0941-2948/2011/0285>
560
- Russell, R. J. (1931). *Dry climates of the United States: I. Climatic map* (Vol. 5): University of California press.
- Sanderson, M. (1999). The Classification of Climates from Pythagoras to Koeppen. *Bulletin of the American Meteorological Society*, 80(4), 669–673. [https://doi.org/10.1175/1520-0477\(1999\)080<0669:TCOCFP>2.0.CO;2](https://doi.org/10.1175/1520-0477(1999)080<0669:TCOCFP>2.0.CO;2)
- Schempp, W., Zeller, K., & Duchon, J. (Eds.) (1977). *Splines minimizing rotation-invariant semi-norms in Sobolev spaces: Constructive Theory of Functions of Several Variables*: Springer Berlin Heidelberg.
565
- Sun, Q., Miao, C., Duan, Q., Ashouri, H., Sorooshian, S., & Hsu, K.-L. (2018). A review of global precipitation data sets: Data sources, estimation, and intercomparisons. *Reviews of Geophysics*, 56(1), 79–107. <https://doi.org/10.1002/2017RG000574>
- Tapiador, F. J., Moreno, R., & Navarro, A. (2019). Consensus in climate classifications for present climate and global warming scenarios. *Atmospheric Research*, 216, 26–36. <https://doi.org/10.1016/j.atmosres.2018.09.017>
570
- Tarkan, A. S., & Vilizzi, L. (2015). Patterns, latitudinal clines and countergradient variation in the growth of roach *Rutilus rutilus* (Cyprinidae) in its Eurasian area of distribution. *Reviews in Fish Biology and Fisheries*, 25(4), 587–602. <https://doi.org/10.1007/s11160-015-9398-6>



- 575 Taylor, K. E., Stouffer, R. J., & Meehl, G. A. (2012). An overview of CMIP5 and the experiment design. *Bulletin of the American Meteorological Society*, 93(4), 485–498. <https://doi.org/10.1175/BAMS-D-11-00094.1>
- Tererai, F., & Wood, A. R. (2014). On the present and potential distribution of *Ageratina adenophora* (Asteraceae) in South Africa. *South African Journal of Botany*, 95, 152–158. <https://doi.org/10.1016/j.sajb.2014.09.001>
- Thornthwaite, C. W. (1931). The climates of North America: According to a new classification. *Geographical Review*, 21(4), 633. <https://doi.org/10.2307/209372>
- 580 Thuiller, W., Lavorel, S., Araújo, M. B., Sykes, M. T., & Prentice, I. C. (2005). Climate change threats to plant diversity in Europe. *Proceedings of the National Academy of Sciences of the United States of America*, 102(23), 8245–8250. <https://doi.org/10.1073/pnas.0409902102>
- Walter, S. D., & Elwood, J. M. (1975). A test for seasonality of events with a variable population at risk. *Journal of Epidemiology & Community Health*, 29(1), 18–21. <https://doi.org/10.1136/jech.29.1.18>
- 585 Wang, M., & Overland, J. E. (2004). Detecting Arctic climate change using Köppen climate classification. *Climatic Change*, 67(1), 43–62. <https://doi.org/10.1007/s10584-004-4786-2>
- Webber, B. L., Yates, C. J., Le Maitre, D. C., Scott, J. K., Kriticos, D. J., Ota, N., . . . Midgley, G. F. (2011). Modelling horses for novel climate courses: Insights from projecting potential distributions of native and alien Australian acacias with correlative and mechanistic models. *Diversity and Distributions*, 17(5), 978–1000. <https://doi.org/10.1111/j.1472-4642.2011.00811.x>
- 590 Willmott, C. J., & Matsuura, K. (2001). Terrestrial air temperature and precipitation: monthly and annual time series (1950 - 1999). Retrieved from http://climate.geog.udel.edu/~climate/html_pages/README.ghcn_ts2.html.
- Winsberg, E. (2012). Values and uncertainties in the predictions of global climate models. *Kennedy Institute of Ethics Journal*, 22(2), 111–137. <https://doi.org/10.1353/ken.2012.0008>
- 595 Yoo, J., & Rohli, R. V. (2016). Global distribution of Köppen–Geiger climate types during the Last Glacial Maximum, Mid-Holocene, and present. *Palaeogeography, Palaeoclimatology, Palaeoecology*, 446, 326–337. <https://doi.org/10.1016/j.palaeo.2015.12.010>